

Equivariant Symmetries for Inertial Navigation Systems

Alessandro Fornasier ^{a,*}, Yixiao Ge ^b, Pieter van Goor ^b, Robert Mahony ^b,
Stephan Weiss ^a

^aControl of Networked Systems Group, University of Klagenfurt, Austria

^bSystem Theory and Robotics Lab, Australian Centre for Robotic Vision, Australian National University, Australia

Abstract

This paper investigates the problem of inertial navigation system (INS) filter design through the lens of symmetry. The extended Kalman filter (EKF) and its variants have been the staple of INS filtering for 50 years. However, recent advances in inertial navigation systems have exploited matrix Lie group structure to design stochastic filters and state observers that have been shown to display superior performance compared to classical solutions. In this work, we explore various symmetries of inertial navigation system, including two novel symmetries that have not been considered in the prior literature, and provide a discussion of the relative strengths and weaknesses of these symmetries in the context of filter design. We show that all the modern variants of the EKF for inertial navigation can be interpreted as the recently proposed equivariant filter (EqF) design methodology applied to different choices of symmetry group for the INS problem. As a direct application of the symmetries presented, we address the filter design problem for a vehicle equipped with an inertial measurement unit (IMU) and a global navigation satellite system (GNSS) receiver, providing a comparative analysis of different modern filter solutions. We believe the collection of symmetries that we present here capture all the sensible choices of symmetry for this problem, and that the analysis provided is indicative of the relative real-world performance potential of the different algorithms for trajectories ensuring full state observability.

Key words: Inertial navigation system; Symmetry; Equivariance; Equivariant filter.

1 Introduction

The theory of invariant filtering for group affine systems [4, 2] and the theory of equivariant filters [18, 21, 28] that generalizes to systems on homogeneous spaces have provided general design frameworks, as well as strong theoretical performance guarantees, for filter designs that exploit symmetry. This has motivated the widespread use of invariant filters in the robotics community, and its adoption for inertial navigation problems [13, 24, 17]. The application of these principles to inertial navigation systems (INS) has seen the most significant performance gains from algorithm design in this field for the last 40 years. There are now several competing modern INS filters based on geometric insights available in the literature [1, 4, 11] and the question of how to analyse and evaluate the similarities and differ-

ences is now of interest. A recent paper by Barrau et al. states “*The big question when it comes to invariant observers/filters is how do we find a group structure for the state space [...]*” [4]. The goal of the present paper is to convince the reader that the choice of symmetry structure is in fact the *only* difference between different versions of modern geometric INS filters.

In this paper we present six different symmetry groups that act on the state-space of the INS problem. We use the recent equivariant filter design methodology to generate INS filter algorithms for each of these symmetries. We show that the classical multiplicative extended Kalman filter (MEKF) [15], the Imperfect-invariant extended Kalman filter (IEKF) [1], the two-frames group invariant extended Kalman filter (TFG-IEKF) [4], and the authors own recent work proposing an equivariant filter for the tangent group structure (TG-EqF) [11] are all associated with equivariant filter design [29] applied to different symmetry actions on the same state-space. This leads us to consider the properties of the symmetry groups and suggests two additional symmetries leading to filters, that we term the Direct Position Equivariant Filter (DP-EqF) and Semi-Direct Bias Equivariant Fil-

* Corresponding author

Email addresses: alessandro.fornasier@aau.at (Alessandro Fornasier), yixiao.ge@anu.edu.au (Yixiao Ge), pieter.vangoor@anu.edu.au (Pieter van Goor), robert.mahony@anu.edu.au (Robert Mahony), stephan.weiss@aau.at (Stephan Weiss).

ter (SD-EqF), that are novel and do not correspond to prior algorithms in the literature.

In the context of GNSS-based navigation, we derive EqF algorithms for all of the different symmetries, demonstrating that this approach provides a unifying analysis framework for modern INS filters. In doing this we also make a minor contribution in demonstrating how fixed-frame measurements can be reformulated as body-frame relative measurements. This allows us to exploit output equivariance [29] for all the filter geometries, ensuring at least third-order linearization error in the output equations.

We undertake a simple comparative study in concert with a linearization analysis of the error equations. We consider the “fully observable” case where all states are estimated and are observable for the given system trajectories. We recognise that for specific cases where trajectories lead to unobservable states (e.g., straight-line flight, hovering, etc.) some of the following observations may not hold. For such trajectories we make the following observations:

- The classical MEKF demonstrates noticeable performance limitations compared to the modern filters. In particular, it demonstrates worse transient response and reports significant overconfidence during the transient phase.
- The performance differences in modern filters are primarily visible during the transient phase of error response. The asymptotic behaviour of all filters is similar.
- Notwithstanding the above, the asymptotic performance of the TG-EqF appears superior to all other filters demonstrating the best consistency and the lowest error.
- The TG-EqF filter is the only filter with exact linearization of the navigation states; the only nonlinearities occur in the bias states. The authors believe that this property underlies its performance advantage.
- The bias state transient response of the filters with semi-direct bias symmetry (TG-EqF, DP-EqF and SD-EqF) appears superior to that of filters without this geometric structure (MEKF, IEKF and TFG-IEKF).

The study concludes that any of the IEKF, TG-EqF, DP-EqF, and SD-EqF filters are candidates for a high-performance INS filter design. The lower filter error and energy properties of the TG-EqF recommend it as the leading choice for fully observable trajectories.

2 Notation and Preliminaries

In this paper bold lowercase letters are used to indicate vector quantities. Bold capital letters are used to indi-

cate matrices. Regular letters are used to indicate elements of a symmetry group.

Frames of reference are denoted as $\{A\}$ and $\{B\}$. Vectors describing physical quantities expressed in a frame of reference $\{A\}$ are denoted by ${}^A\mathbf{x}$. Rotation matrices encoding the orientation of a frame of reference $\{B\}$ with respect to a reference $\{A\}$ are denoted by ${}^A\mathbf{R}_B$; in particular, ${}^A\mathbf{R}_B$ expresses a vector ${}^B\mathbf{x}$ defined in the $\{B\}$ frame of reference into a vector ${}^A\mathbf{x} = {}^A\mathbf{R}_B {}^B\mathbf{x}$ expressed in the $\{A\}$ frame of reference. Finally, $\mathbf{I}_n \in \mathbb{R}^{n \times n}$ is the $n \times n$ identity matrix, and $\mathbf{0}_{n \times m} \in \mathbb{R}^{n \times m}$ is the $n \times m$ zero matrix.

For all $\mathbf{x} \in \mathbb{R}^n$ define the maps:

$$\begin{aligned} \overline{(\cdot)} : \mathbb{R}^n &\rightarrow \mathbb{R}^{n+3}, & \mathbf{x} &\mapsto \overline{\mathbf{x}} = (\mathbf{0}_{3 \times 1}, \mathbf{x}), \\ \underline{(\cdot)} : \mathbb{R}^n &\rightarrow \mathbb{R}^{n+3}, & \mathbf{x} &\mapsto \underline{\mathbf{x}} = (\mathbf{x}, \mathbf{0}_{3 \times 1}). \end{aligned}$$

The following Lie groups are used throughout the paper.

$$\begin{aligned} \mathbf{SO}(3) &= \{ \mathbf{A} \in \mathbb{R}^{3 \times 3} \mid \mathbf{A}\mathbf{A}^\top = \mathbf{I}_3, \det(\mathbf{A}) = 1 \}, \\ \mathbf{SE}(3) &= \left\{ \begin{bmatrix} \mathbf{A} & \mathbf{b} \\ \mathbf{0}_{1 \times 3} & 1 \end{bmatrix} \in \mathbb{R}^{4 \times 4} \mid \mathbf{A} \in \mathbf{SO}(3), \mathbf{b} \in \mathbb{R}^3 \right\}, \\ \mathbf{SE}_2(3) &= \left\{ \begin{bmatrix} \mathbf{A} & \mathbf{a} & \mathbf{b} \\ \mathbf{0}_{1 \times 3} & 1 & 0 \\ \mathbf{0}_{1 \times 3} & 0 & 1 \end{bmatrix} \in \mathbb{R}^{5 \times 5} \mid \mathbf{A} \in \mathbf{SO}(3), \mathbf{a}, \mathbf{b} \in \mathbb{R}^3 \right\}. \end{aligned}$$

Their Lie algebras are the tangent spaces at the identities of each group.

For all $X = (\mathbf{A}, \mathbf{a}, \mathbf{b}) \in \mathbf{SE}_2(3) \mid \mathbf{A} \in \mathbf{SO}(3), \mathbf{a}, \mathbf{b} \in \mathbb{R}^3$, define the map:

$$\Omega(\cdot) : \mathbf{SE}_2(3) \rightarrow \mathfrak{se}_2(3), \quad \Omega(X) = (\mathbf{0}_{3 \times 1}, \mathbf{0}_{3 \times 1}, \mathbf{a})^\wedge \in \mathfrak{se}_2(3).$$

For all $\mathbf{p}, \mathbf{q}, \mathbf{r} \in \mathbb{R}^3 \mid (\mathbf{p}, \mathbf{q}, \mathbf{r}) \in \mathbb{R}^9$, define the map:

$$\Pi(\cdot) : \mathfrak{se}_2(3) \rightarrow \mathfrak{se}(3), \quad \Pi((\mathbf{p}, \mathbf{q}, \mathbf{r})^\wedge) = (\mathbf{p}, \mathbf{q})^\wedge \in \mathfrak{se}(3).$$

In what follows, we recall the concept of symmetry, equivariance, and equivariant filter design. For an introduction to Lie groups and homogeneous spaces in the context of equivariant filter, we refer the reader to the authors’ prior work [18, 20, 29, 11]. The appendix B also provides additional explanation.

2.1 Symmetry Equivariance and Lifted System

A symmetry of a kinematic system can be seen as a set of transformations that either leave unchanged or change

in a structured manner the equations that govern the motion of the system. This is encoded by a transitive group action ϕ of a Lie group \mathbf{G} (also called a *symmetry group*) on the state space \mathcal{M} of a system. Formally, a (right) Lie group action $\phi : \mathbf{G} \times \mathcal{M} \rightarrow \mathcal{M}$ is a smooth map satisfying

$$\phi(XY, \xi) = \phi(Y, \phi(X, \xi)), \quad \phi(I, \xi) = \xi,$$

for all $X, Y \in \mathbf{G}$ and $\xi \in \mathcal{M}$. An action ϕ is said to be *transitive* if for all $\xi_1, \xi_2 \in \mathcal{M}$, there exists $X \in \mathbf{G}$ such that $\phi(X, \xi_1) = \xi_2$.

A symmetry that transforms the equations of motion of a kinematic system in a structured manner encodes *equivariance* of the system. Formally, consider a system $f : \mathbb{L} \rightarrow \mathfrak{X}(\mathcal{M})$ as a map from a vector space of inputs \mathbb{L} to vector fields on the state space \mathcal{M} ; that is, each input $u \in \mathbb{L}$ corresponds to a vector field $f_u \in \mathfrak{X}(\mathcal{M})$ on the state space \mathcal{M} . Then f is said to be *equivariant* if

$$d\phi_X \circ f_u \circ \phi_{X^{-1}} = f_{\psi_X(u)}, \quad (1)$$

$\forall X \in \mathbf{G}$, $u \in \mathbb{L}$, and for a right-handed group action $\psi : \mathbf{G} \times \mathbb{L} \rightarrow \mathbb{L}$ of the group \mathbf{G} on the input space \mathbb{L} . Similarly, a symmetry that changes the output in a structured manner encodes *equivariance of the output*. Formally, consider an output map $h : \mathcal{M} \rightarrow \mathcal{N}$ where \mathcal{N} is a smooth manifold called the output space. Then h is said to be *equivariant* if

$$h(\phi_X(\xi)) = \rho_X(h(\xi)), \quad (2)$$

$\forall X \in \mathbf{G}$, $\xi \in \mathcal{M}$, and for a right-handed action of the group \mathbf{G} on the output space \mathcal{N} , that is $\rho : \mathbf{G} \times \mathcal{N} \rightarrow \mathcal{N}$.

Note that for any fixed $X \in \mathbf{G}$ the actions ϕ, ψ and ρ can be written as diffeomorphisms $\phi_X : \mathcal{M} \rightarrow \mathcal{M}$, $\psi_X : \mathbb{L} \rightarrow \mathbb{L}$ and $\rho_X : \mathcal{N} \rightarrow \mathcal{N}$.

If a system possesses a symmetry (\mathbf{G}, ϕ) , the Lie group structure of the symmetry group can be exploited to “lift” the system dynamics on the Lie group. That is, with an arbitrary but fixed choice of origin point $\hat{\xi} \in \mathcal{M}$, defining a geometric structure called “Lift” $\Lambda : \mathcal{M} \times \mathbb{L} \rightarrow \mathfrak{g}$ and defining a *lifted system* $\dot{\hat{X}} = X\Lambda(\phi_X(\hat{\xi}), u)$ whose solutions $\hat{X}(t)$ at time t , project to solutions $\xi(t)$ [18, 29].

2.2 Equivariant Filter Design

For state estimation problems, lifting the system dynamics onto the Lie group translates the problem to that of estimating an element of the symmetry group $\hat{X} \in \mathbf{G}$ such that $\hat{\xi} = \phi(\hat{X}, \hat{\xi})$, rather than $\hat{\xi} \in \mathcal{M}$ directly. This is not just an “embedding” of the system on the Lie group, but abstracts the estimation problem to the Lie group.

Exploiting the symmetry of the kinematic systems allows the definition of a *global error* $e = \phi(\hat{X}^{-1}, \xi) \in \mathcal{M}$, termed *equivariant error* [29, 27]. The EqF is then the state estimation algorithm that results from applying EKF design principles to the (global) error kinematics, linearized about the fixed origin $\hat{\xi}$.

Let $f : \mathbb{L} \rightarrow \mathfrak{X}(\mathcal{M})$ be a system whose state space is a m -dimensional homogeneous space \mathcal{M} , and let $h : \mathcal{M} \rightarrow \mathcal{N}$ be an output function where the output space is a n -dimensional smooth manifold \mathcal{N} . Assume that f and h are equivariant as in Section 2.1. Let $\xi(t) \in \mathcal{M}$ be a trajectory of the system with measurements,

$$\dot{\xi} = f_u(\xi), \quad y(t_k) = h(\xi(t_k)),$$

where $u(t) \in \mathbb{L}$ is a measured input signal, and the measurements $y(t_k) \in \mathcal{N}$ occur at discrete times $t_1 < t_2 < \dots$. Choose a fixed origin $\hat{\xi} \in \mathcal{M}$ and let $\Lambda : \mathcal{M} \times \mathbb{L} \rightarrow \mathfrak{g}$ be a lift of the system. Let $\hat{X} \in \mathbf{G}$ denote the observer state and define its dynamics to be

$$\dot{\hat{X}} = \hat{X}\Lambda(\phi(\hat{X}, \hat{\xi}), u), \quad \hat{X}(t_k^+) = \exp(\Delta(t_k))\hat{X}(t_k^+),$$

where the $\Delta(t_k) \in \mathfrak{g}$ are correction terms that depend on the measurements $y(t_k)$.

The *equivariant error* is defined to be $e := \phi_{\hat{X}^{-1}}(\xi)$. Choose local coordinates of the state space $\vartheta : \mathcal{U}_{\hat{\xi}} \rightarrow \mathbb{R}^m$ in a neighbourhood $\mathcal{U}_{\hat{\xi}} \subset \mathcal{M}$ of $\hat{\xi}$, and choose local coordinates of the output space $\delta : \mathcal{U}_{\hat{y}} \rightarrow \mathbb{R}^n$ in a neighbourhood $\mathcal{U}_{\hat{y}} \subset \mathcal{N}$ of $\hat{y} = h(\hat{\xi})$. Let $\varepsilon = \vartheta(e)$ denote the local coordinates of the error e . Then the linearized error dynamics and linearized output are [28]

$$\begin{aligned} \dot{\varepsilon} &\approx \mathbf{A}_t^0 \varepsilon, \\ \mathbf{A}_t^0 &= D_e|_{\hat{\xi}} \vartheta(e) D_E|_I \phi_{\hat{\xi}}(E) D_e|_{\hat{\xi}} \Lambda(e, \hat{u}) D_\varepsilon|_0 \vartheta^{-1}(\varepsilon), \\ \delta(h(e)) &= \delta(h(\rho(\hat{X}^{-1}, y))) \approx \mathbf{C}^0 \varepsilon, \\ \mathbf{C}^0 &= D_y|_{\hat{y}} \delta(y) D_e|_{\hat{\xi}} h(e) D_\varepsilon|_0 \vartheta^{-1}(\varepsilon). \end{aligned}$$

If no compatible action ψ of the symmetry group on the input space is found, the state matrix can be computed alternatively according to

$$\begin{aligned} \mathbf{A}_t^0 &= D_e|_{\hat{\xi}} \vartheta(e) D_\xi|_{\hat{\xi}} \phi_{\hat{X}^{-1}}(\xi) D_E|_I \phi_{\hat{\xi}}(E) \\ &\quad D_\xi|_{\phi_X(\hat{\xi})} \Lambda(\xi, u) D_e|_{\hat{\xi}} \phi_{\hat{X}}(e) D_\varepsilon|_0 \vartheta^{-1}(\varepsilon). \end{aligned}$$

Output equivariance can be exploited to derive a linearized output with third order error [29] as follows

$$\begin{aligned} \delta(h(e)) &= \delta(\rho_{\hat{X}^{-1}}(h(\xi))) \approx \mathbf{C}^* \varepsilon + \mathbf{O}(\varepsilon^3), \\ \mathbf{C}^* \varepsilon &= \frac{1}{2} D_y|_{\hat{y}} \delta(y) (D_E|_I \rho_E(\hat{y}) + D_E|_I \rho_E(\rho_{\hat{X}^{-1}}(y))) \varepsilon^\wedge. \end{aligned}$$

Let \mathbf{C} be either \mathbf{C}^0 or \mathbf{C}^* , then the EqF algorithm is

Predict:

$$\begin{aligned}\dot{\hat{X}} &= \text{dL}_{\hat{X}} \Lambda(\phi_{\hat{\xi}}(\hat{X}), u), \\ \dot{\Sigma} &= \mathbf{A}_t^0 \Sigma + \Sigma \mathbf{A}_t^{0\top} + \mathbf{Q},\end{aligned}$$

Update:

$$\begin{aligned}\Delta &= \text{D}_E|_I \phi_{\hat{\xi}}(E)^\dagger \text{d}\vartheta^{-1} \Sigma \mathbf{C}^\top (\mathbf{C} \Sigma \mathbf{C}^\top + \mathbf{R})^{-1} \delta(\rho(\hat{X}^{-1}, y)), \\ \Sigma &= (\mathbf{I} - \Sigma \mathbf{C}^\top (\mathbf{C} \Sigma \mathbf{C}^\top + \mathbf{R})^{-1} \mathbf{C}) \Sigma, \\ \hat{X} &= \exp(\Delta) \hat{X},\end{aligned}$$

Reset:

$$\Sigma = \exp(\Gamma_{\text{d}\phi_{\hat{\xi}} \Delta}) \Sigma \exp(\Gamma_{\text{d}\phi_{\hat{\xi}} \Delta})^\top.$$

where the last equation (Reset) accounts for the distortion of the covariance due to the change of coordinate maps on a non-flat manifold, and is often referred to as *reset step* or *curvature correction* [20, 12].

The equations above resemble those of continuous-discrete Kalman-like filters, and indeed, the EqF has the same order of computational complexity as any other Kalman-like filter, such as EKF and MEKF.

3 Outline of the Paper

The paper is organized as follows. Section 4 introduces the biased inertial navigation system considered. Section 5 introduces and analyzes different symmetries of the biased inertial navigation system under the lens of equivariance. That is, for each symmetry, its equivariance properties, as well as the relation to classical filter design when exploited within the equivariant filter framework, are discussed. In particular, Tab. 2 provides an summary of the different symmetries considered, with its rightmost column showing the linearized error dynamics when these symmetries are exploited for filter design. Section 6 describes how the linearization error analysis is carried out. For readers who do not wish to replicate the straightforward but tedious calculations required to compute the linearisations, the detailed derivations are provided in the appendix B. Section 7 discussed the problem of unmanned aerial vehicle (UAV) position-based localization as a direct application of the symmetries presented in Section 5. This application serves as a convenient framework to introduce an interesting result in Section 7.1. That is, how global-referenced measurements are reformulated as residual body-referenced measurements that are compatible with the presented symmetries. Finally, Section 7 concludes with an experimental validation of the performance of the different equivariant filters built upon the symmetries discussed in Section 5.

4 The Biased Inertial Navigation Problem

Consider a mobile robot equipped with an IMU providing angular velocity and acceleration measurements, as well as other sensors providing partial direct or indirect state measurements (e.g. a GNSS receiver providing position measurements or a magnetometer providing direction measurements). Let $\{G\}$ denote the global inertial frame of reference and $\{I\}$ denote the IMU frame of reference. In non-rotating, flat earth assumption, the deterministic (noise-free) continuous-time biased inertial navigation system is

$${}^G \dot{\mathbf{R}}_I = {}^G \mathbf{R}_I ({}^I \boldsymbol{\omega} - {}^I \mathbf{b}_\omega)^\wedge, \quad (3a)$$

$${}^G \dot{\mathbf{v}}_I = {}^G \mathbf{R}_I ({}^I \mathbf{a} - {}^I \mathbf{b}_a) + {}^G \mathbf{g}, \quad (3b)$$

$${}^G \dot{\mathbf{p}}_I = {}^G \mathbf{v}_I, \quad (3c)$$

$${}^I \dot{\mathbf{b}}_\omega = {}^I \boldsymbol{\tau}_\omega, \quad (3d)$$

$${}^I \dot{\mathbf{b}}_a = {}^I \boldsymbol{\tau}_a. \quad (3e)$$

Here, ${}^G \mathbf{R}_I$ denotes the rigid body orientation, and ${}^G \mathbf{p}_I$ and ${}^G \mathbf{v}_I$ denote the rigid body position and velocity expressed in the $\{G\}$ frame, respectively. These variables are termed the *navigation states*. The gravity vector ${}^G \mathbf{g}$ is expressed in frame $\{G\}$. The gyroscope measurement and accelerometer measurement are written ${}^I \boldsymbol{\omega}$ and ${}^I \mathbf{a}$ respectively. The two biases ${}^I \mathbf{b}_\omega$ and ${}^I \mathbf{b}_a$ are termed the *bias states*. The inputs $\boldsymbol{\tau}_\omega$, $\boldsymbol{\tau}_a$ are used to model the biases' dynamics, and are zero when the biases are modeled as constant quantities.

The state space is $\mathcal{M} = \mathcal{SO}(3) \times \mathbb{R}^3 \times \mathbb{R}^3 \times \mathbb{R}^3 \times \mathbb{R}^3$ where the 4 copies of \mathbb{R}^3 model velocity, position, and angular and acceleration bias, respectively, and $\mathcal{SO}(3)$ is the $\mathbf{SO}(3)$ -torsor with rotation matrices representing coordinates of orientation rather than physical rotation of space. Note that the state space itself is not a Lie-group in the EqF formulation. Rather symmetry is modeled as a group action on \mathcal{M} , allowing us to consider different symmetries acting on the same INS state. We write an element of the state space, and an element of the input space respectively

$$\xi = ({}^G \mathbf{R}_I, {}^G \mathbf{v}_I, {}^G \mathbf{p}_I, {}^I \mathbf{b}_\omega, {}^I \mathbf{b}_a) \in \mathcal{M}, \quad (4)$$

$$u = ({}^I \boldsymbol{\omega}, {}^I \mathbf{a}, {}^I \boldsymbol{\tau}_\omega, {}^I \boldsymbol{\tau}_a) \in \mathbb{L} \subset \mathbb{R}^{12}. \quad (5)$$

For the sake of clarity of the presentation, in the following sections, we drop subscripts and superscripts from state, input and output variables, and adopt the lean notation defined in Table 1.

5 INS Symmetries

Starting with Tab. 2, we show the relation between INS filters and symmetry group, as well as the differences in

Table 1
Descriptive-Lean Notation Conversion Table.

Description	Descriptive notation	Lean notation
Rigid body orientation	${}^G\mathbf{R}_I$	\mathbf{R}
Rigid body velocity	${}^G\mathbf{v}_I$	\mathbf{v}
Rigid body position	${}^G\mathbf{p}_I$	\mathbf{p}
Angular velocity measurement	${}^I\boldsymbol{\omega}$	$\boldsymbol{\omega}$
Gyroscope bias	${}^I\mathbf{b}_\omega$	\mathbf{b}_ω
Acceleration measurement	${}^I\mathbf{a}$	\mathbf{a}
Accelerometer bias	${}^I\mathbf{b}_a$	\mathbf{b}_a

the state error linearization of filters built upon those symmetries. In Sec. 5.1, 5.2 and 5.3, we discuss the symmetry groups that lead to the design of equivariant filters equivalent to the widely-known MEKF, IEKF, and the recently published TFG-IEKF. In Sec. 5.4 we briefly recall the tangent group recently introduced and exploited for INS in our prior work [11, 10]. In Sec. 5.5 and 5.6, we introduce two new symmetry groups for biased inertial navigation Systems. These groups are based on the semi-direct product and aim to address the over-parametrization of bias states introduced in our prior work [11].

5.1 Special Orthogonal group $\mathbf{G}_O : \mathbf{SO}(3) \times \mathbb{R}^{12}$

Lie group theory was first applied to navigation systems to overcome the limitation and the singularities of using Euler angles as the parameterization of the attitude of a rigid body. Originally formulated on the quaternion group, the modern approach directly models attitude on the Special Orthogonal group $\mathbf{SO}(3)$.

Define the symmetry group $\mathbf{G}_O := \mathbf{SO}(3) \times \mathbb{R}^{12}$, and let $X = (A, a, b, \alpha, \beta) \in \mathbf{G}_O$, where $A \in \mathbf{SO}(3)$, $a, b, \alpha, \beta \in \mathbb{R}^3$. Let $X = (A_X, a_X, b_X, \alpha_X, \beta_X)$, $Y = (A_Y, a_Y, b_Y, \alpha_Y, \beta_Y)$ be two elements of the symmetry group, then the group product is written $XY = (A_X A_Y, a_X + a_Y, b_X + b_Y, \alpha_X + \alpha_Y, \beta_X + \beta_Y)$. The inverse of an element X is given by $X^{-1} = (A^\top, -a, -b, -\alpha, -\beta)$.

Lemma 1 Define $\phi : \mathbf{G}_O \times \mathcal{M} \rightarrow \mathcal{M}$ as

$$\phi(X, \xi) := (\mathbf{R}A, \mathbf{v} + a, \mathbf{p} + b, \mathbf{b}_\omega + \alpha, \mathbf{b}_a + \beta) \in \mathcal{M}. \quad (6)$$

Then, ϕ is a transitive right group action of \mathbf{G}_O on \mathcal{M} .

The existence of a transitive group action of the symmetry group \mathbf{G}_O on the state space \mathcal{M} guarantees the existence of a lift [18].

Theorem 2 Define the map $\Lambda : \mathcal{M} \times \mathbb{L} \rightarrow \mathfrak{go}$ by

$$\Lambda(\xi, u) := (\Lambda_1(\xi, u), \dots, \Lambda_5(\xi, u)).$$

where $\Lambda_1 : \mathcal{M} \times \mathbb{L} \rightarrow \mathfrak{so}(3)$, and $\Lambda_2, \dots, \Lambda_5 : \mathcal{M} \times \mathbb{L} \rightarrow \mathbb{R}^3$ are given by

$$\Lambda_1(\xi, u) := ({}^I\boldsymbol{\omega} - {}^I\mathbf{b}_\omega)^\wedge, \quad (7)$$

$$\Lambda_2(\xi, u) := {}^G\mathbf{R}_I ({}^I\mathbf{a} - {}^I\mathbf{b}_a) + {}^G\mathbf{g}, \quad (8)$$

$$\Lambda_3(\xi, u) := {}^G\mathbf{v}_I, \quad (9)$$

$$\Lambda_4(\xi, u) := {}^I\boldsymbol{\tau}_\omega, \quad (10)$$

$$\Lambda_5(\xi, u) := {}^I\boldsymbol{\tau}_a. \quad (11)$$

Then, the Λ is a lift for the system in Equ. (3) with respect to the symmetry group $\mathbf{G}_O := \mathbf{SO}(3) \times \mathbb{R}^{12}$.

In the appendix B, it is shown that an EqF designed using this symmetry results in the well-known MEKF [15].

5.2 Extended Special Euclidean group $\mathbf{G}_{ES} : \mathbf{SE}_2(3) \times \mathbb{R}^6$

Using the extended pose $\mathbf{SE}_2(3)$ group to model the navigation states of the INS problem is one of the major developments in INS filtering in the last 10 years.

Define $\xi = (\mathbf{T}, \mathbf{b}) \in \mathcal{M} := \mathcal{SE}_2(3) \times \mathbb{R}^6$ to be the state space of the system. $\mathbf{T} = (\mathbf{R}, \mathbf{v}, \mathbf{p}) \in \mathcal{SE}_2(3)$ is the extended pose [6], which includes the orientation the, velocity and the position of the rigid body, whereas $\mathbf{b} = (\mathbf{b}_\omega, \mathbf{b}_a) \in \mathbb{R}^6$ denotes the IMU biases. Let $u = (\mathbf{w}, \boldsymbol{\tau}) \in \mathbb{L} \subseteq \mathbb{R}^{12}$ denote the system input, where $\mathbf{w} = (\boldsymbol{\omega}, \mathbf{a}) \in \mathbb{R}^6$ denotes the input given by the IMU readings, and $\boldsymbol{\tau} = (\boldsymbol{\tau}_\omega, \boldsymbol{\tau}_a) \in \mathbb{R}^6$ denotes the input for the IMU biases. Define the matrices

$$\begin{aligned} \mathbf{G} &= (\underline{\mathbf{g}})^\wedge \in \mathfrak{se}_2(3), \\ \mathbf{B} &= (\underline{\mathbf{b}})^\wedge \in \mathfrak{se}_2(3), \quad \mathbf{N} = \begin{bmatrix} \mathbf{0}_{3 \times 3} & \mathbf{0}_{3 \times 1} & \mathbf{0}_{3 \times 1} \\ \mathbf{0}_{1 \times 3} & 0 & 1 \\ \mathbf{0}_{1 \times 3} & 0 & 0 \end{bmatrix} \in \mathbb{R}^{5 \times 5}. \\ \mathbf{W} &= (\underline{\mathbf{w}})^\wedge \in \mathfrak{se}_2(3), \end{aligned}$$

Then, the system in Equ. (3) may then be written as

$$\dot{\mathbf{T}} = \mathbf{T}(\mathbf{W} - \mathbf{B} + \mathbf{N}) + (\mathbf{G} - \mathbf{N})\mathbf{T}, \quad (12a)$$

$$\dot{\mathbf{b}} = \boldsymbol{\tau}. \quad (12b)$$

Define the symmetry group $\mathbf{G}_{ES} := \mathbf{SE}_2(3) \times \mathbb{R}^6$, and let $X = (C, \gamma) \in \mathbf{G}_{ES}$, where $C = (A, a, b) \in \mathbf{SE}_2(3)$, $A \in \mathbf{SO}(3)$, $a, b \in \mathbb{R}^3$, $\gamma \in \mathbb{R}^6$. Let $X = (C_X, \gamma_X)$, $Y = (C_Y, \gamma_Y)$ be two elements of the symmetry group, then the group product is written $XY = (C_X C_Y, \gamma_X + \gamma_Y)$. The inverse of an element X is given by $X^{-1} = (C^{-1}, -\gamma)$.

² The homogeneous Galilean group $\mathbf{HG}(3)$ is isomorphic to $\mathbf{SE}(3)$ but acts on attitude and velocity rather than attitude and position.

Table 2

Qualitative overview of the differences in the presented symmetries when exploited for filter design. The first column indicates the filter that is obtained by applying equivariant filter design methodology with the symmetry in the second column. The third column describes the features of the state error linearization for the specific filter, whereas the rightmost column shows the linearized error dynamics. For readers that do not have time to compute the linearisations themselves, detailed derivations are provided in appendix B

Filter	Symmetry group	State error linearization.	$\mathbf{A} \mid \dot{\boldsymbol{\varepsilon}} \simeq \mathbf{A} \boldsymbol{\varepsilon}$
MEKF [15]	Special Orthogonal group $\mathbf{G}_O : \mathbf{SO}(3) \times \mathbb{R}^{12}$	State-dependent attitude error dynamics. State-dependent and input-dependent velocity error dynamics. Linear time-invariant position error dynamics. Linear time-invariant bias error dynamics	$\dot{\boldsymbol{\varepsilon}}_R \simeq -\hat{\mathbf{R}} \boldsymbol{\varepsilon}_{b_\omega} + \mathcal{O}(\boldsymbol{\varepsilon}^2),$ $\dot{\boldsymbol{\varepsilon}}_v \simeq -(\hat{\mathbf{R}}(\mathbf{a} - \hat{\mathbf{b}}_a))^\wedge \boldsymbol{\varepsilon}_R - \hat{\mathbf{R}} \boldsymbol{\varepsilon}_{b_a} + \mathcal{O}(\boldsymbol{\varepsilon}^2),$ $\dot{\boldsymbol{\varepsilon}}_p \simeq \boldsymbol{\varepsilon}_v,$ $\dot{\boldsymbol{\varepsilon}}_b = \mathbf{0}.$
Imperfect-IEKF [1]	Extended Special Euclidean group $\mathbf{G}_{ES} : \mathbf{SE}_2(3) \times \mathbb{R}^6$	State-dependent attitude, position and velocity error dynamics. Linear time-invariant bias error dynamics	$\dot{\boldsymbol{\varepsilon}}_R \simeq -\hat{\mathbf{R}} \boldsymbol{\varepsilon}_{b_\omega} + \mathcal{O}(\boldsymbol{\varepsilon}^2),$ $\dot{\boldsymbol{\varepsilon}}_v \simeq \mathbf{g}^\wedge \boldsymbol{\varepsilon}_R - \hat{\mathbf{v}}^\wedge \hat{\mathbf{R}} \boldsymbol{\varepsilon}_{b_\omega} - \hat{\mathbf{R}} \boldsymbol{\varepsilon}_{b_a} + \mathcal{O}(\boldsymbol{\varepsilon}^2),$ $\dot{\boldsymbol{\varepsilon}}_p \simeq \boldsymbol{\varepsilon}_v - \hat{\mathbf{p}}^\wedge \hat{\mathbf{R}} \boldsymbol{\varepsilon}_{b_\omega} + \mathcal{O}(\boldsymbol{\varepsilon}^2),$ $\dot{\boldsymbol{\varepsilon}}_b = \mathbf{0}.$
TFG-IEKF [4]	Two-Frames group $\mathbf{G}_{TF} : \mathbf{SO}(3) \times (\mathbb{R}^6 \oplus \mathbb{R}^6)$	Linear time-invariant attitude error dynamics. State-dependent velocity and position error dynamics. State-dependent and input-dependent bias error dynamics	$\dot{\boldsymbol{\varepsilon}}_R \simeq -\boldsymbol{\varepsilon}_{b_\omega},$ $\dot{\boldsymbol{\varepsilon}}_v \simeq \mathbf{g}^\wedge \boldsymbol{\varepsilon}_R - \hat{\mathbf{v}}^\wedge \boldsymbol{\varepsilon}_{b_\omega} - \boldsymbol{\varepsilon}_{b_a} + \mathcal{O}(\boldsymbol{\varepsilon}^2),$ $\dot{\boldsymbol{\varepsilon}}_p \simeq \boldsymbol{\varepsilon}_v - \hat{\mathbf{p}}^\wedge \boldsymbol{\varepsilon}_{b_\omega} + \mathcal{O}(\boldsymbol{\varepsilon}^2),$ $\dot{\boldsymbol{\varepsilon}}_{b_\omega} \simeq (\hat{\mathbf{R}}(\boldsymbol{\omega} - \hat{\mathbf{b}}_\omega))^\wedge \boldsymbol{\varepsilon}_{b_\omega} + \mathcal{O}(\boldsymbol{\varepsilon}^2),$ $\dot{\boldsymbol{\varepsilon}}_{b_a} \simeq (\hat{\mathbf{R}}(\boldsymbol{\omega} - \hat{\mathbf{b}}_\omega))^\wedge \boldsymbol{\varepsilon}_{b_a} + \mathcal{O}(\boldsymbol{\varepsilon}^2).$
TG-EqF [11]	Tangent group $\mathbf{G}_{TG} : \mathbf{SE}_2(3) \times \mathfrak{se}_2(3)$	Linear time-invariant attitude, velocity and position error dynamics. State-dependent and input-dependent bias error dynamics	$\dot{\boldsymbol{\varepsilon}}_R \simeq \boldsymbol{\varepsilon}_{b_\omega},$ $\dot{\boldsymbol{\varepsilon}}_v \simeq \mathbf{g}^\wedge \boldsymbol{\varepsilon}_R + \boldsymbol{\varepsilon}_{b_a},$ $\dot{\boldsymbol{\varepsilon}}_p \simeq \boldsymbol{\varepsilon}_v + \boldsymbol{\varepsilon}_{b_\nu},$ $\dot{\boldsymbol{\varepsilon}}_b \simeq \mathbf{ad}_{(\hat{\mathbf{w}}^\wedge + \mathbf{G})}^\vee \boldsymbol{\varepsilon}_b + \mathcal{O}(\boldsymbol{\varepsilon}^2).$
DP-EqF	Direct Position group ² $\mathbf{G}_{DP} : \mathbf{HG}(3) \times \mathfrak{hg}(3) \times \mathbb{R}^3$	Linear time-invariant attitude and velocity error dynamics. State-dependent and input-dependent position and bias error dynamics	$\dot{\boldsymbol{\varepsilon}}_R \simeq \boldsymbol{\varepsilon}_{b_\omega},$ $\dot{\boldsymbol{\varepsilon}}_v \simeq \mathbf{g}^\wedge \boldsymbol{\varepsilon}_R + \boldsymbol{\varepsilon}_{b_a},$ $\dot{\boldsymbol{\varepsilon}}_p \simeq \boldsymbol{\varepsilon}_v - \hat{\mathbf{v}}^\wedge \boldsymbol{\varepsilon}_R + \mathcal{O}(\boldsymbol{\varepsilon}^2),$ $\dot{\boldsymbol{\varepsilon}}_b \simeq \mathbf{ad}_{(\hat{\mathbf{w}}^\wedge + \mathbf{G})}^\vee \boldsymbol{\varepsilon}_b + \mathcal{O}(\boldsymbol{\varepsilon}^2).$
SD-EqF	Semi-Direct Bias group $\mathbf{G}_{SD} : \mathbf{SE}_2(3) \times \mathfrak{se}(3)$	Linear time-invariant attitude and velocity error dynamics. State-dependent position error dynamics. State-dependent and input-dependent bias error dynamics	$\dot{\boldsymbol{\varepsilon}}_R \simeq \boldsymbol{\varepsilon}_{b_\omega},$ $\dot{\boldsymbol{\varepsilon}}_v \simeq \mathbf{g}^\wedge \boldsymbol{\varepsilon}_R + \boldsymbol{\varepsilon}_{b_a},$ $\dot{\boldsymbol{\varepsilon}}_p \simeq \boldsymbol{\varepsilon}_v + \hat{\mathbf{p}}^\wedge \boldsymbol{\varepsilon}_{b_\omega} + \mathcal{O}(\boldsymbol{\varepsilon}^2),$ $\dot{\boldsymbol{\varepsilon}}_b \simeq \mathbf{ad}_{(\hat{\mathbf{w}}^\wedge + \mathbf{G})}^\vee \boldsymbol{\varepsilon}_b + \mathcal{O}(\boldsymbol{\varepsilon}^2).$

Lemma 3 Define $\phi : \mathbf{G}_{ES} \times \mathcal{M} \rightarrow \mathcal{M}$ as

$$\phi(X, \xi) := (\mathbf{T}C, \mathbf{b} + \gamma) \in \mathcal{M}. \quad (13)$$

Then, ϕ is a transitive right group action of \mathbf{G}_{ES} on \mathcal{M} .

Theorem 4 Define the map $\Lambda : \mathcal{M} \times \mathbb{L} \rightarrow \mathfrak{g}_{ES}$ by

$$\Lambda(\xi, u) := (\Lambda_1(\xi, u), \Lambda_2(\xi, u)),$$

where $\Lambda_1 : \mathcal{M} \times \mathbb{L} \rightarrow \mathfrak{se}_2(3)$, and $\Lambda_2 : \mathcal{M} \times \mathbb{L} \rightarrow \mathbb{R}^6$ are given by

$$\Lambda_1(\xi, u) := (\mathbf{W} - \mathbf{B} + \mathbf{N}) + \mathbf{T}^{-1}(\mathbf{G} - \mathbf{N})\mathbf{T}, \quad (14)$$

$$\Lambda_2(\xi, u) := \boldsymbol{\tau}. \quad (15)$$

Then, Λ is a lift for the system in Equ. (12) with respect to the symmetry group $\mathbf{G}_{ES} := \mathbf{SE}_2(3) \times \mathbb{R}^6$.

Applying the EqF filter design methodology to this symmetry leads to the Imperfect-IEKF [1, 2]. Note that ignoring the bias and considering only the navigation states is the original IEKF filter [1]. The imperfect term comes from breaking the group-affine symmetry of the navigation states by adding the direct product terms for the bias.

5.3 Two-Frames group: $\mathbf{G}_{TF} : \mathbf{SO}(3) \times (\mathbb{R}^6 \oplus \mathbb{R}^6)$

The recently published two-frames group invariant extended Kalman filter [4] is one approach to address the

theoretical issue in the imperfect IEKF for INS where the bias terms are not part of the symmetry structure.

Consider the system in Equ. (12). Define the symmetry group $\mathbf{G}_{\mathbf{TF}} := \mathbf{SO}(3) \ltimes (\mathbb{R}^6 \oplus \mathbb{R}^6)$, where $\mathbf{SO}(3)$ acts on two vector spaces of 6 dimensions each defined with respect to two different frames of references. Let $X = (C, \gamma) \in \mathbf{G}_{\mathbf{TF}}$, with $C = (A, (a, b)) \in \mathbf{SE}_2(3) := \mathbf{SO}(3) \ltimes \mathbb{R}^6$ such that $A \in \mathbf{SO}(3)$, $(a, b) \in \mathbb{R}^6$. Let, $*$: $\mathbf{SO}(3) \times \mathbb{R}^{3N} \rightarrow \mathbb{R}^{3N}$ be the rotation term introduced in [4], such that $\forall A \in \mathbf{SO}(3)$ and $x = (x_1, \dots, x_N) \in \mathbb{R}^{3N}$, $A * x = (Ax_1, \dots, Ax_N)$. Define the group product $XY = (C_X C_Y, \gamma_X + A_X * \gamma_Y)$. The inverse element of the symmetry group writes $X^{-1} = (C^{-1}, -A^T * \gamma) \in \mathbf{G}_{\mathbf{TF}}$.

Lemma 5 Define $\phi : \mathbf{G}_{\mathbf{TF}} \times \mathcal{M} \rightarrow \mathcal{M}$ as

$$\phi(X, \xi) := (\mathbf{T}C, A^T * (\mathbf{b} - \gamma)) \in \mathcal{M}. \quad (16)$$

Then, ϕ is a transitive right group action of $\mathbf{G}_{\mathbf{TF}}$ on \mathcal{M} .

Theorem 6 Define $\Lambda_1 : \mathcal{M} \times \mathbb{L} \rightarrow \mathfrak{se}_2(3)$ as

$$\Lambda_1(\xi, u) := (\mathbf{W} - \mathbf{B} + \mathbf{N}) + \mathbf{T}^{-1}(\mathbf{G} - \mathbf{N})\mathbf{T}, \quad (17)$$

define $\Lambda_2 : \mathcal{M} \times \mathbb{L} \rightarrow \mathbb{R}^6$ as

$$\Lambda_2(\xi, u) := (\mathbf{b}_\omega^\wedge(\omega - \mathbf{b}_\omega) - \tau_\omega, \mathbf{b}_a^\wedge(\omega - \mathbf{b}_\omega) - \tau_a). \quad (18)$$

Then, the map $\Lambda(\xi, u) = (\Lambda_1(\xi, u), \Lambda_2(\xi, u))$ is a lift for the system in Equ. (12) with respect to the symmetry group $\mathbf{G}_{\mathbf{TF}} := \mathbf{SO}(3) \ltimes (\mathbb{R}^6 \oplus \mathbb{R}^6)$.

In the appendix B, it is shown that designing and EqF based on this symmetry leads to the recently published TFG-IEKF [4].

5.4 Tangent group $\mathbf{G}_{\mathbf{TG}} : \mathbf{SE}_2(3) \ltimes \mathfrak{se}_2(3)$

Recent work [23, 22] considered symmetries and EqF filter design on the tangent group \mathbf{TG} of a general Lie-group. Since bias states are closely related to velocities, these ideas can easily be extended symmetries for bias states [11].

Define $\xi = (\mathbf{T}, \mathbf{b}) \in \mathcal{M} := \mathcal{SE}_2(3) \times \mathbb{R}^9$ to be the state space of the system. $\mathbf{T} \in \mathcal{SE}_2(3)$ represents the extended pose, whereas $\mathbf{b} = (\mathbf{b}_\omega, \mathbf{b}_a, \mathbf{b}_\nu) \in \mathbb{R}^9$ represents the IMU biases, and an additional virtual bias \mathbf{b}_ν . Let $u = (\mathbf{w}, \boldsymbol{\tau}) \in \mathbb{L} \subseteq \mathbb{R}^{18}$ denote the system input, where $\mathbf{w} = (\omega, \mathbf{a}, \boldsymbol{\nu}) \in \mathbb{R}^9$ denotes the input given by the IMU readings, and an additional virtual input $\boldsymbol{\nu}$. Note that we can set $\boldsymbol{\nu} = \mathbf{b}_\nu$ such that the original dynamics in Equ. (3) are recovered. $\boldsymbol{\tau} = (\tau_\omega, \tau_a, \tau_\nu) \in \mathbb{R}^9$ denotes the

input for the IMU biases. Define the matrices

$$\begin{aligned} \mathbf{G} &= (\bar{\mathbf{g}})^\wedge \in \mathfrak{se}_2(3), \\ \mathbf{B} &= \mathbf{b}^\wedge \in \mathfrak{se}_2(3), \quad \mathbf{N} = \begin{bmatrix} \mathbf{0}_{3 \times 3} & \mathbf{0}_{3 \times 1} & \mathbf{0}_{3 \times 1} \\ \mathbf{0}_{1 \times 3} & 0 & 1 \\ \mathbf{0}_{1 \times 3} & 0 & 0 \end{bmatrix} \in \mathbb{R}^{5 \times 5}. \\ \mathbf{W} &= \mathbf{w}^\wedge \in \mathfrak{se}_2(3), \end{aligned}$$

With these newly defined matrices, the system in Equ. (3) may then be written in compact form as in Equ. (12). Note, however, that the matrices \mathbf{B} and \mathbf{W} are different than those in Equ. (12).

Define the symmetry group $\mathbf{G}_{\mathbf{TG}} := \mathbf{SE}_2(3) \ltimes \mathfrak{se}_2(3)$, and let $X = (C, \gamma) \in \mathbf{G}_{\mathbf{TG}}$, where $C \in \mathbf{SE}_2(3)$, $\gamma \in \mathfrak{se}_2(3)$. Let $X = (C_X, \gamma_X)$, $Y = (C_Y, \gamma_Y)$ be two elements of the symmetry group, then the group product is written $XY = (C_X C_Y, \gamma_X + \text{Ad}_{C_X}[\gamma_Y])$. The inverse of an element X is given by $X^{-1} = (C^{-1}, -\text{Ad}_{C^{-1}}[\gamma])$.

Lemma 7 Define $\phi : \mathbf{G}_{\mathbf{TG}} \times \mathcal{M} \rightarrow \mathcal{M}$ as

$$\phi(X, \xi) := (\mathbf{T}C, \text{Ad}_{C^{-1}}^\vee(\mathbf{b} - \gamma^\vee)) \in \mathcal{M}. \quad (19)$$

Then, ϕ is a transitive right group action of $\mathbf{G}_{\mathbf{TG}}$ on \mathcal{M} .

From here, we derive a compatible action of the symmetry group $\mathbf{G}_{\mathbf{TG}}$ on the input space \mathbb{L} and derive the lift Λ via constructive design as described in [18, 28].

Lemma 8 Define $\psi : \mathbf{G}_{\mathbf{TG}} \times \mathbb{L} \rightarrow \mathbb{L}$ as

$$\psi(X, u) := (\text{Ad}_{C^{-1}}^\vee(\mathbf{w} - \gamma^\vee) + \Omega^\vee(C^{-1}), \text{Ad}_{C^{-1}}^\vee \boldsymbol{\tau}) \in \mathbb{L}. \quad (20)$$

Then, ψ is a right group action of $\mathbf{G}_{\mathbf{TG}}$ on \mathbb{L} .

The system in Equ. (12) is equivariant under the actions ϕ in Equ. (19) and ψ in Equ. (20). The existence of a transitive group action of the symmetry group $\mathbf{G}_{\mathbf{TG}}$ on the state space \mathcal{M} and the equivariance of the system guarantees the existence of an equivariant lift [18].

Theorem 9 Define the map $\Lambda : \mathcal{M} \times \mathbb{L} \rightarrow \mathfrak{g}_{\mathbf{TG}}$ by

$$\Lambda(\xi, u) := (\Lambda_1(\xi, u), \Lambda_2(\xi, u)),$$

where $\Lambda_1 : \mathcal{M} \times \mathbb{L} \rightarrow \mathfrak{se}_2(3)$, and $\Lambda_2 : \mathcal{M} \times \mathbb{L} \rightarrow \mathfrak{se}_2(3)$ are given by

$$\Lambda_1(\xi, u) := (\mathbf{W} - \mathbf{B} + \mathbf{N}) + \mathbf{T}^{-1}(\mathbf{G} - \mathbf{N})\mathbf{T}, \quad (21)$$

$$\Lambda_2(\xi, u) := \text{ad}_b[\Lambda_1(\xi, u)] - \boldsymbol{\tau}^\wedge. \quad (22)$$

Then, Λ is an equivariant lift for the system in Equ. (12) with respect to the symmetry group $\mathbf{G}_{\mathbf{TG}} := \mathbf{SE}_2(3) \ltimes \mathfrak{se}_2(3)$.

This approach requires the introduction of a new state \mathbf{b}_ν in order to apply the full $\mathfrak{se}_2(3)$ semi-direct symmetry on the bias states. This new state is entirely virtual, it does not exist in the real system. Since introducing an entirely virtual state just for the sake of the symmetry appears questionable, it is of interest to consider alternative symmetries that try to preserve the semi-direct group structure that models bias interaction, but doesn't require the additional bias filter state.

5.5 Direct Position group $\mathbf{G}_{\text{DP}} : \mathbf{HG}(3) \ltimes \mathfrak{hg}(3) \times \mathbb{R}^3$

In this subsection, we investigate a symmetry that does not require the over-parametrization of the state introduced in [11] given by the addition of a velocity bias state. Specifically, we achieve this by considering a semi-direct product symmetry only on the homogeneous Galilean structure of the state space and an Euclidean symmetry for the position state.

We introduce the term $\mathbf{HG}(3)$ for the *homogeneous Galilean* group. This corresponds to extended pose transformations $\mathbf{SE}_2(3)$ where the spatial translation is zero. That is the symmetry acts on rotation and velocity only with the semi-direct product induced by the $\mathbf{SE}_2(3)$ geometry. The homogeneous Galilean group is isomorphic to $\mathbf{SE}(3)$ in structure, however, since $\mathbf{SE}(3)$ is synonymous with pose transformation we use the $\mathbf{HG}(3)$ notation to avoid confusion.

The first step towards these goals is to introduce a virtual input ν and rewrite Equ. (3c) as $\dot{\mathbf{p}} = \mathbf{R}\nu + \mathbf{v}$. Note that the input ν can be set to zero to recover the original dynamics in Equ. (3).

Define $\xi = (\mathbf{T}, \mathbf{p}, \mathbf{b}) \in \mathcal{M} := \mathcal{HG}(3) \times \mathbb{R}^3 \times \mathbb{R}^6$ to be the state space of the system, where $\mathbf{T} = (\mathbf{R}, \mathbf{v}) \in \mathcal{HG}(3)$ includes the orientation and the velocity of the rigid body. Let $u = (\mathbf{w}, \nu, \tau) \in \mathbb{L} \subseteq \mathbb{R}^{15}$ denote the system input. Define the matrices

$$\mathbf{G} = (\bar{\mathbf{g}})^\wedge \in \mathfrak{se}(3), \quad \mathbf{B} = \mathbf{b}^\wedge \in \mathfrak{se}(3), \quad \mathbf{W} = \mathbf{w}^\wedge \in \mathfrak{se}(3).$$

Then, the system in Equ. (3) may then be written as

$$\dot{\mathbf{T}} = \mathbf{T}(\mathbf{W} - \mathbf{B}) + \mathbf{G}\mathbf{T}, \quad (23a)$$

$$\dot{\mathbf{p}} = \mathbf{R}\nu + \mathbf{v}, \quad (23b)$$

$$\dot{\mathbf{b}} = \tau. \quad (23c)$$

Define the symmetry group $\mathbf{G}_{\text{DP}} := \mathbf{HG}(3) \ltimes \mathfrak{se}(3) \times \mathbb{R}^3$, and let $X = (B, \beta, c) \in \mathbf{G}_{\text{DP}}$ with $B = (A, a) \in \mathbf{HG}(3)$ such that $A \in \mathbf{SO}(3)$, $a \in \mathbb{R}^3$. Let $X = (B_X, \beta_X, c_X)$, $Y = (B_Y, \beta_Y, c_Y) \in \mathbf{G}_{\text{DP}}$, the group product is written $XY = (B_X B_Y, \beta_X + \text{Ad}_{B_X}[\beta_Y], c_X + c_Y)$. The inverse of an element $X \in \mathbf{G}_{\text{DP}}$ is given by $X^{-1} = (B^{-1}, -\text{Ad}_{B^{-1}}[\beta], -c) \in \mathbf{G}_{\text{DP}}$.

Lemma 10 Define $\phi : \mathbf{G}_{\text{DP}} \times \mathcal{M} \rightarrow \mathcal{M}$ as

$$\phi(X, \xi) := (\mathbf{T}B, \text{Ad}_{B^{-1}}^\vee(\mathbf{b} - \beta^\vee), \mathbf{p} + c) \in \mathcal{M}. \quad (24)$$

Then, ϕ is a transitive right group action of \mathbf{G}_{DP} on \mathcal{M} .

We derive a compatible action of the symmetry group \mathbf{G}_{DP} on the input space \mathbb{L} .

Lemma 11 Define $\psi : \mathbf{G}_{\text{DP}} \times \mathbb{L} \rightarrow \mathbb{L}$ as

$$\psi(X, u) := (\text{Ad}_{B^{-1}}^\vee(\mathbf{w} - \beta^\vee), A^T(\nu - a), \text{Ad}_{B^{-1}}^\vee \tau) \in \mathbb{L}. \quad (25)$$

Then, ψ is a right group action of \mathbf{G}_{DP} on \mathbb{L} .

The system in Equ. (23) is equivariant under the actions ϕ in Equ. (24) and ψ in Equ. (25). Therefore, the existence of an equivariant lift is guaranteed.

Theorem 12 Define the map $\Lambda : \mathcal{M} \times \mathbb{L} \rightarrow \mathfrak{g}_{\text{DP}}$ by

$$\Lambda(\xi, u) := (\Lambda_1(\xi, u), \Lambda_2(\xi, u), \Lambda_3(\xi, u)),$$

where $\Lambda_1 : \mathcal{M} \times \mathbb{L} \rightarrow \mathfrak{hg}(3)$, $\Lambda_2 : \mathcal{M} \times \mathbb{L} \rightarrow \mathfrak{se}(3)$, and $\Lambda_3 : \mathcal{M} \times \mathbb{L} \rightarrow \mathbb{R}^3$ are given by

$$\Lambda_1(\xi, u) := (\mathbf{W} - \mathbf{B}) + \mathbf{T}^{-1}\mathbf{G}\mathbf{T}, \quad (26)$$

$$\Lambda_2(\xi, u) := \text{ad}_{\mathbf{b}^\wedge}[\Lambda_1(\xi, u)] - \tau^\wedge, \quad (27)$$

$$\Lambda_3(\xi, u) := \mathbf{R}\nu + v. \quad (28)$$

Then, the Λ is an equivariant lift for the system in Equ. (23) with respect to the symmetry group $\mathbf{G}_{\text{DP}} := \mathbf{HG}(3) \ltimes \mathfrak{hg}(3) \times \mathbb{R}^3$.

The symmetry proposed in this subsection allows for a minimal state parametrization (i.e. absence of over-parametrization of the state with additional state variables). However, the construction comes at the cost of separating the position state from the geometric $\mathbf{SE}_2(3)$ structure and modeling it as a direct product linear space.

5.6 Semi-Direct Bias group: $\mathbf{G}_{\text{SD}} : \mathbf{SE}_2(3) \ltimes \mathfrak{se}(3)$

In this subsection, we investigate a symmetry that maintains a minimal state representation (not requiring the introduction of an additional velocity bias state) while keeping the position state within the geometric structure given by $\mathbf{SE}_2(3)$.

Consider the system in Equ. (12). Define the symmetry group $\mathbf{G}_{\text{SD}} := \mathbf{SE}_2(3) \ltimes \mathfrak{se}(3)$ with group product $XY = (C_X C_Y, \gamma_X + \text{Ad}_{C_X}[\gamma_Y])$ for $X = (C_X, \gamma_X)$, $Y = (C_Y, \gamma_Y) \in \mathbf{G}_{\text{SD}}$. Here, for $X = (C, \gamma) \in \mathbf{G}_{\text{SD}}$ one has $C = (A, a, b) = (B, b) \in \mathbf{SE}_2(3)$ such that

$A \in \mathbf{SO}(3)$, $a, b \in \mathbb{R}^3$, and $B = (A, a) \in \mathbf{HG}(3)$. The element $C \in \mathbf{SE}_2(3)$ in its matrix representation is written

$$C = \begin{bmatrix} A & a & b \\ \mathbf{0}_{1 \times 3} & 1 & 0 \\ \mathbf{0}_{1 \times 3} & 0 & 1 \end{bmatrix} = \begin{bmatrix} B & b \\ \dots & 0 \\ \mathbf{0}_{1 \times 3} & 0 & 1 \end{bmatrix} \in \mathbf{SE}_2(3).$$

The inverse element is written

$$X^{-1} = (C^{-1}, -\text{Ad}_{B^{-1}}[\gamma]) \in \mathbf{G}_{\text{SD}}.$$

Lemma 13 Define $\phi : \mathbf{G}_{\text{SD}} \times \mathcal{M} \rightarrow \mathcal{M}$ as

$$\phi(X, \xi) := (\mathbf{T}C, \text{Ad}_{B^{-1}}^\vee(b - \gamma^\vee)) \in \mathcal{M}. \quad (29)$$

Then, ϕ is a transitive right group action of \mathbf{G}_{SD} on \mathcal{M} .

Theorem 14 Define $\Lambda_1 : \mathcal{M} \times \mathbb{L} \rightarrow \mathfrak{se}_2(3)$ as

$$\Lambda_1(\xi, u) := (\mathbf{W} - \mathbf{B} + \mathbf{N}) + \mathbf{T}^{-1}(\mathbf{G} - \mathbf{N})\mathbf{T}, \quad (30)$$

define $\Lambda_2 : \mathcal{M} \times \mathbb{L} \rightarrow \mathfrak{se}(3)$ as

$$\Lambda_2(\xi, u) := \text{ad}_{b^\wedge}[\Pi(\Lambda_1(\xi, u))] - \tau^\wedge, \quad (31)$$

Then, the map $\Lambda(\xi, u) = (\Lambda_1(\xi, u), \Lambda_2(\xi, u))$ is a lift for the system in Equ. (12) with respect to the symmetry group $\mathbf{G}_{\text{SD}} := \mathbf{SE}_2(3) \ltimes \mathfrak{se}(3)$.

The symmetry proposed in this subsection is a variation of the symmetry defined in our previous work [11] that does not require over-parametrization of the state and additional state variables.

6 Linearization Error Analysis

In Sec. 5, we present different symmetry groups for the inertial navigation problem. An indicator of the performance of an EqF with a particular symmetry is the order of approximation error in the associated linearization of error dynamics.

For all symmetries, the origin $\hat{\xi} \in \mathcal{M}$ is chosen to be $\hat{\xi} := (\hat{\mathbf{R}}, \hat{\mathbf{v}}, \hat{\mathbf{p}}, \hat{\mathbf{b}}_\omega, \hat{\mathbf{b}}_a) = (\mathbf{I}_3, \mathbf{0}_{3 \times 1}, \mathbf{0}_{3 \times 1}, \mathbf{0}_{3 \times 1}, \mathbf{0}_{3 \times 1})$. Define the local coordinate chart $\vartheta : \mathcal{U}_{\hat{\xi}} \rightarrow \mathbb{R}^n$, to be

$$\vartheta := (\phi_{\hat{\xi}} \cdot \exp_{\mathbf{G}})^{-1} = \log_{\mathbf{G}} \cdot \phi_{\hat{\xi}}^{-1}, \quad (32)$$

on a neighborhood of $\hat{\xi} \in \mathcal{M}$ such that $\log_{\mathbf{G}} \cdot \phi_{\hat{\xi}}^{-1}$ is bijective. The chart ϑ is always well-defined locally since all group actions considered are free. The local error coordinates are defined by $\varepsilon := \vartheta(e)$, so long as $e := \phi(\hat{X}^{-1}, \xi)$ remains in the domain of definition of ϑ .

In Equ. (32), $\log_{\mathbf{G}}$ denotes the log coordinates on the symmetry group considered. This map is different for each symmetry group. For a product Lie group $\mathbf{G} := \mathbf{G}_1 \times \mathbf{G}_2$, the logarithm is given by $\log_{\mathbf{G}}((A, B)) = (\log_{\mathbf{G}_1}(A), \log_{\mathbf{G}_2}(B))$. When the product groups are Lie groups with well-known exponential maps, then the standard expressions are used [8]. For the semi-direct product groups $\mathbf{G} \ltimes \mathfrak{g}$ where \mathfrak{g} is the Lie algebra of \mathbf{G} , we will use a matrix realization to compute the exponential and the logarithm algebraically.

In the rightmost column of Tab. 2, we present the linearization of the state error dynamics associated with each of the symmetries considered. The linearization is expressed in terms of elements $\varepsilon = \log(E) \in \mathfrak{g}$ where the element $E \in \mathbf{G}$ corresponds bijectively to the error $e \in \mathcal{M}$ through the free group action. That is, we solve

$$\text{D}\vartheta^{-1}(\varepsilon)[\dot{\varepsilon}] \approx \frac{d}{dt}e = f(\vartheta^{-1}(\varepsilon), u)$$

for $\dot{\varepsilon}$ to first order in ε . Here $\dot{e} = f(e, u)$ is the full error dynamics expressed as a function of e and the input u [20, 29]. Finally, the filter design follows the procedure outlined in Sec. 2 and in the authors' earlier works [29, 20, 11, 10]. The detailed derivation of the error linearization for each symmetry, as well as the related equivariant filters, are provided in the appendix B.

Barrau and Bonnabel [1] developed the IEKF for the bias free INS problem and showed that the linearization of the navigation states was exact. This was a significant improvement on the MEKF geometry, where the linearization of the navigation states is not exact, independently of the bias. However, this exact linearization property is lost when bias is added to the INS problem, the system is no longer group affine [2]. Using a direct product geometric structure to add bias leads to the Imperfect-IEKF [2] and introduces linearization error in the navigation state equations (cf. Tab. 2). The remaining filters all model coupling between bias and navigation states using semi-direct geometry of some form or other. The TG-EqF is the only filter for which the linearization of the navigation state is exact. In this case, the linearization error is only present in the bias states. The DP-EqF, SD-EqF and TFG-IEKF all have semi-direct geometric coupling between part of their navigation states and the bias states leading to exact or improved linearization where the coupling acts compatibly with the TG structure.

7 Application: position-based localization

In the present section, we discuss a practical application of the symmetries presented in Sec. 5, that is UAV position-based localization.

Consider the system in Equ. (3), and consider the output for global position measurements:

$$h(\xi) = \mathbf{p} \in \mathbb{R}^3. \quad (33)$$

It is straightforward to verify the $\mathbf{G}_{\mathbf{ES}}, \mathbf{G}_{\mathbf{TG}}, \mathbf{G}_{\mathbf{SD}}, \mathbf{G}_{\mathbf{TF}}$ symmetries do not possess output equivariance [28, 29] for global position measurements directly.

7.1 Reformulation of position measurements as equivariant

Here, we show how position measurements can be reformulated as residual body-frame measurements imposing a nonlinear constraint [14]. The modified measurement is output equivariant with respect to a suitable group action, and the linearization methodology proposed in [29] can be applied to generate cubic linearization error in the output.

Lemma 15 *Let π be a measurement of global position. Define a new measurement model $h(\xi) \in \mathbb{R}^3$, describing the body-referenced difference between the measured global position and the position state as follows*

$$h(\xi) = \mathbf{R}^T(\pi - \mathbf{p}) \in \mathbb{R}^3. \quad (34)$$

Let $y = h(\xi) \in \mathcal{N}$ be a measurement defined according to the above model in Equ. (34), define $\rho : \mathbf{G} \times \mathbb{R}^3 \rightarrow \mathbb{R}^3$ such that

$$\rho_X(y) := A^T(y - b). \quad (35)$$

Then, the output defined in Equ. (34) is equivariant.

The noise-free value for y is zero and the output innovation $\delta(\rho_{\hat{X}^{-1}}(\mathbf{0})) = \rho_{\hat{X}^{-1}}(\mathbf{0}) - \pi$ measures the mismatch of the observer state in reconstructing the true state up to noise in the raw measurement π .

7.2 Experimental evaluation

We document results from a suite of experiments chosen to provide a comparison of the performance of the MEKF, the Imperfect-IEKF, the TFG-IEKF, an EqF based on the $\mathbf{G}_{\mathbf{TG}}$ symmetry [11] termed TG-EqF, an EqF based on the $\mathbf{G}_{\mathbf{DP}}$ symmetry termed DP-EqF, and an EqF based on the $\mathbf{G}_{\mathbf{SD}}$ symmetry termed SD-EqF. Moreover, given the global nature of the measurement, we included in the comparison a left-sided Imperfect-IEKF which directly uses the measurement in Equ. (33). Note that each of the aforementioned EqFs have been implemented including the reset step discussed in Sec. 2, whereas the Imperfect-IEKFs and the TFG-IEKF have been implemented without reset step, according to their original implementation, discussed in [1, 4] respectively. We undertake two separate experimental analyses. In the first experiment, we undertake a Monte-Carlo simulation of an UAV equipped with an IMU receiving acceleration and angular velocity measurements at 200Hz and

receiving global position measurements at 10Hz, simulating a GNSS receiver. In the second experiment, we compare all the filters with real data from the INSANE dataset [5].

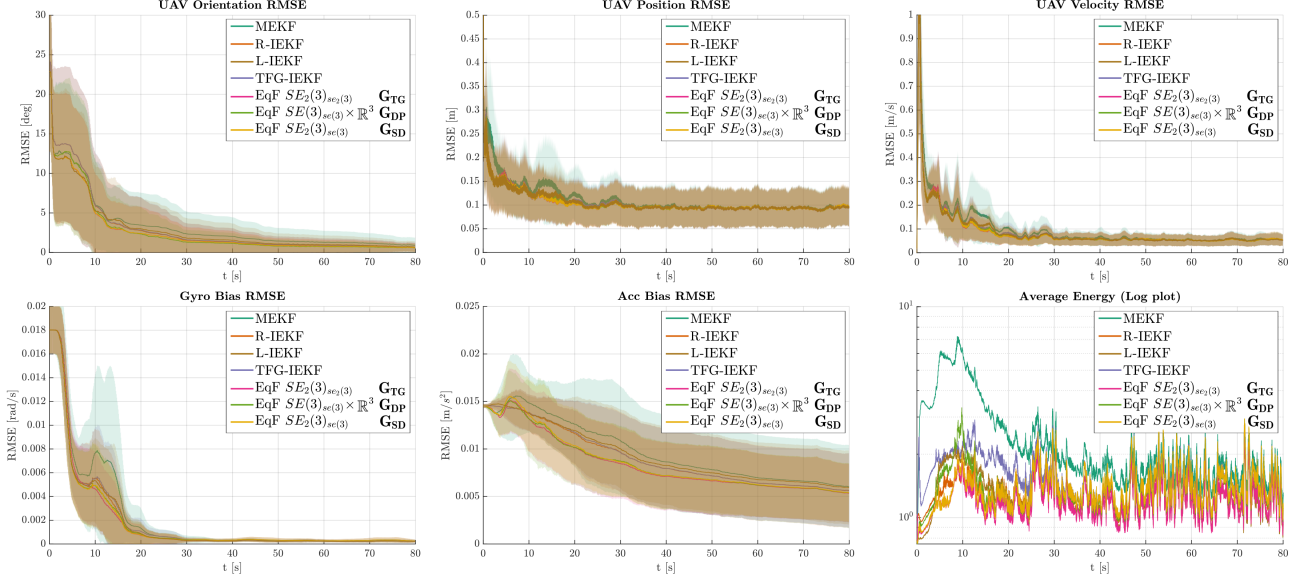
7.3 UAV Flight Simulation

In this experiment, we conducted a Monte-Carlo simulation, including four hundred runs of a simulated UAV equipped with an IMU and receiving global position measurements simulating a GNSS receiver. In order to simulate realistic flight conditions, we selected the initial 80s from four sequences in the Euroc dataset's vicon room [7] as reference trajectories. For each sequence, we generated a hundred runs, incorporating synthetic IMU data generated interpolating and differentiating the Vicon poses, and position measurements while varying the initial conditions for the position (distributed normally around zero with 1m standard deviation per axis) and the attitude (distributed normally around zero with 20° standard deviation per axis). This experiment considers common realistic condition. For application of the semi-direct product symmetries in scenarios of difficult alignment we refer the reader to the authors' related work [11, 10, 25, 9].

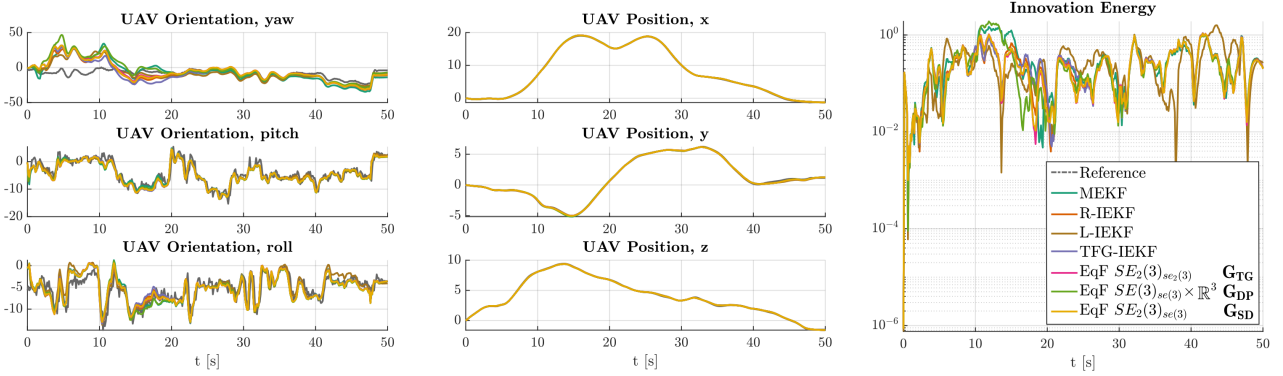
The ground truth IMU biases are randomly generated every run following a Gaussian distribution with standard deviation of 0.01rad/s \sqrt{s} for the gyro bias and 0.01m/s \sqrt{s} for the accelerometer bias. To simulate realistic global position measurement, additive Gaussian noise with a standard deviation of 0.2m per axis is added.

For a fair comparison, we were careful to use the same prior distributions and noise parameters for all filters. This includes accounting for the different scaling and transformations of noise due to the input and state parametrizations for the different geometries. Similarly, each filter shares the same input and output measurement noise covariance adapted to the particular geometry of the filter. The validity of the noise models can be verified in the Average Energy plot (Fig. 1a), which plots the average normalized estimation error squared (ANEES) [16]. Here, all filters initialize with unity ANEES, demonstrating that the prior sampling and observer response corresponds to the stochastic prior used, and all filters converge towards unity ANEES as expected from a filter driven by Gaussian noise. All the filters are initialized at the identity (zero attitude, zero position, zero velocity, and zero biases).

The primary plots in Fig. 1a show the RMSE values for the navigation states (on the top) and the bias states (on the bottom). It is clear that the MEKF filter demonstrates worse performance than the modern geometric filters. There is little difference visible in the transient and asymptotic error response of the navigation states for the modern filters. The remaining attitude error is



(a) Average RMSE and sample variance (shaded) of the filters' states, and full filter energy.



(b) Orientation and position states evolution, and innovation energy for the real-world UAV flight experiment.

Figure 1. Simulation and real-world experiments' results. Orange: R-IEKF. Brown: L-IEKF. Purple: TFG-IEKF. Magenta: TG-EqF. Green: DP-EqF. Yellow: SD-EqF.

due to yaw error. The position and velocity errors converge to the noise limits of the measurement signals. In contrast, there are clear differences visible in the transient response of the bias states. To make the difference in the transient response clearer, Tab. 3, shows the average RMSE values of each filter for the first 30s of the trajectory and the percentage improvement of the geometric filters with respect to the MEKF. Additionally, Tab. 4 shows the time taken by each filter to reach an average RMSE below 10% of the maximum RMSE value. Based on these results, the filters split roughly into three categories: the three filters with semi-direct bias symmetry (TG-EqF, DP-EqF and SD-EqF) which appear to display the best transient response in any state. The IEKFs and TFG-IEKF, which have the $\mathbf{SE}_2(3)$ symmetry but do not use a semi-direct geometry for the bias geometry, have similar bias transient. The accelerometer bias, in particular, is clearly separated from the filters with the

semi-direct group symmetry. Finally, the MEKF which suffers from not modeling the $\mathbf{SE}_2(3)$ symmetry at all.

The average energy plot provides an additional important analysis tool. This plot shows the ANEES [16] defined as

$$\text{ANEES} = \frac{1}{nM} \sum_{i=1}^M \epsilon_i^T \Sigma_i^{-1} \epsilon_i,$$

where ϵ is the specific filter error state, Σ is the error covariance, $M = 400$ is the number of runs in the Monte-Carlo simulation, and n is the dimension of the state space. The ANEES provides a measure of the consistency of the filter estimate. An ANEES of unity means that the observed error variance corresponds exactly to the estimated covariance of the information state. When ANEES is larger than unity, it indicates that the filter is overconfident; that is, the observed error is larger than the estimate of the state covariance predicts. All 'pure'

Table 3

RMSE values and percentage of improvement of the geometric filters with respect to the MEKF for the first 30s of the UAV simulation, corresponding to the transient phase (T). Best values are in **bold**, second best values are underlined. In the table, R-IEKF and L-IEKF represent respectively the right-sided and the left-sided Imperfect-IEKF.

RMSE (T)	MEKF	R-IEKF	L-IEKF	TFG-IEKF	TG-EqF	DP-EqF	SD-EqF
Orientation	0.1108 (100%)	0.1076 (97%)	0.1011 (91%)	0.1082 (98%)	0.0938 (85%)	0.0968 (87%)	<u>0.0939 (85%)</u>
Position	0.1433 (100%)	0.1276 (89%)	0.129 (90%)	0.1290 (90%)	<u>0.1267 (88%)</u>	0.1270 (89%)	0.1263 (88%)
Velocity	0.1728 (100%)	0.1459 (84%)	0.146 (84%)	0.1488 (86%)	<u>0.1411 (82%)</u>	0.1411 (82%)	0.1399 (81%)
Gyro bias	0.0054 (100%)	0.0044 (83%)	0.0045 (83%)	0.0046 (85%)	<u>0.0043 (81%)</u>	0.0043 (81%)	0.0043 (80%)
Acc bias	0.0134 (100%)	0.0125 (94%)	0.013 (95%)	0.0126 (94%)	0.0116 (87%)	<u>0.0117 (88%)</u>	0.0119 (89%)

Table 4

Transient times taken by each filter to reach an average RMSE below 10% of the maximum RMSE value. The accelerometer bias is excluded since the average RMSE never reached a value below 10% of the maximum RMSE value. Best values are in **bold**, second best values are underlined. In the table, R-IEKF and L-IEKF represent respectively the right-sided and the left-sided Imperfect-IEKF.

Transient time	MEKF	R-IEKF	L-IEKF	TFG-IEKF	TG-EqF	DP-EqF	SD-EqF
Orientation	32.090 (100%)	23.095 (72%)	26.595 (83%)	23.995 (75%)	<u>21.295 (66%)</u>	20.395 (64%)	<u>21.295 (66%)</u>
Position	5.095 (100%)	<u>4.795 (94%)</u>	4.595 (90%)	<u>4.795 (94%)</u>	4.995 (98%)	<u>4.795 (94%)</u>	<u>4.795 (94%)</u>
Velocity	16.295 (100%)	12.495 (77%)	15.895 (98%)	12.495 (77%)	12.495 (77%)	<u>12.695 (78%)</u>	12.495 (77%)
Gyro bias	17.095 (100%)	<u>16.095 (94%)</u>	16.395 (96%)	16.295 (95%)	15.895 (93%)	16.195 (95%)	15.895 (93%)

Table 5

ANEES for the first 30s, corresponding to the transient phase (T) and for the remaining of the trajectory length, corresponding to the asymptotic phase (A). Best values are in **bold**, second best values are underlined. In the table, R-IEKF and L-IEKF represent respectively the right-sided and the left-sided Imperfect-IEKF.

ANEES	MEKF	R-IEKF	L-IEKF	TFG-IEKF	TG-EqF	DP-EqF	SD-EqF
Transient (T)	3.11	1.36	1.39	1.71	1.20	1.44	<u>1.32</u>
Asymptotic (A)	1.69	1.40	1.20	1.43	<u>1.22</u>	1.42	1.44

extended Kalman filters tend to be overconfident since their derivation ignores linearization errors in the model. The closer to an ANEES of unity that a filter manages is directly correlated to the consistency of the filter estimate and is usually linked to smaller linearization errors. To provide numeric results, we have averaged the ANEES values over the transient and asymptotic sections of the filter response and presented them in Tab. 5. Here, it is clear that the TG-EqF is superior, with a consistent ANEES for the whole duration of the experiment, the five other filters R-IEKF, L-IEKF, TFG-IEKF, DP-EqF and SD-EqF are similar in the transient phase, with the L-IEKF that improves in the asymptotic phase. Finally, the MEKF is worst. The ANEES of the MEKF diverges to over seven before converging, corresponding to an overconfidence of a factor of seven standard deviations in the state error. Such a level of overconfidence is dangerous in a real-world scenario and may indeed lead to divergence of the filter estimate in certain situations. Note that in practice, overconfidence of a filter is avoided by inflating the process noise model covariance to account for linearization error in the model. A more consistent filter requires a smaller covariance inflation

and has correspondingly more confidence in its model than a filter that is less consistent.

In conclusion, the TG-EqF exhibits the best convergence rate, particularly in orientation and IMU biases, as well as the best consistency of all the filters. Hence, the TG-EqF is the filter we recommend using for INS problems. We believe that this performance can be traced back to the coupling of the IMU bias with the navigation states that are inherent in the semi-direct product structure of the symmetry group $\mathbf{G}_{\mathbf{TG}}$ and the exact linearization of the navigation error dynamics (Tab. 2). Note that the bias states are poorly observable states and possess slow dynamics. Consequently, moving linearization error into these states heuristically appears better than leaving the linearization error in the main navigation states that are much more dynamic.

7.4 Real-world UAV flight

In this experiment, we compared the performance of the discussed filters in a real-world UAV flight scenario from the INSANE dataset [5]. In particular, in this ex-

periment, a quadcopter is flying for 50m at a maximum height of 13m covering an area of roughly 200m², at a maximum speed of 3m/s. The UAV is receiving IMU measurements at 200Hz, as well as measurements from and RTK-GNSS receiver at 8Hz with an accuracy between 0.1m and 0.6m. The position and orientation reference has been obtained as described in [5] from raw sensor measurements of two RTK-GNSS and a magnetometer.

Similar to the previous experiments, all the filters share the same tuning parameters.

Fig. 1b shows the evolution of each filter orientation and position estimates, as well as the innovation energy, commonly referred to as the Normalised Innovation Squared (NIS) error

$$\text{NIS} = \frac{1}{n} \mathbf{r}^T \mathbf{S}^{-1} \mathbf{r},$$

where \mathbf{r} is the specific measurement residual of dimension n computed via the output action ρ and \mathbf{S} is the innovation covariance. The results in Fig. 1b show that the high level conclusions from the simulations are confirmed on real data. There are slight differences between filters in the plotted results but due to the lack of accurate ground truth all that can be deduced is that all the filters provide high quality real-world INS solutions. This is not surprising since the MEKF is the industry standard and is known to perform well in practice and the more modern filters are expected to improve on this performance.

8 Conclusion

This study investigates inertial navigation system filter design from the perspective of symmetry. We establish a unifying framework, demonstrating that various modern INS filter variants can be interpreted as equivariant filters applied to distinct choices of symmetry, with the group structure being the only difference among those filter variants. With specific application to position measurements, we demonstrated that fixed-frame measurements can be reformulated as body-frame relative measurements. This allows one to exploit the equivariance of the output, ensuring third-order linearization error in the measurement equations.

We discussed and presented different symmetry groups acting on the state-space of the INS problem. Novel symmetries are introduced alongside analysis of similarities and differences in the context of filter design. Furthermore, we showed how different choices of symmetries lead to filters with different linearized error dynamics, and how the \mathbf{G}_{TG} symmetry yields exact linearization of the navigation error, shifting all the linearisation error into the bias state dynamics.

Comparative performance studies in simulation, and real-world of a vehicle equipped with an IMU and receiving position measurement from a GNSS receiver highlighted that any of the R-IEKF, L-IEKF, TFG-IEKF, TG-EqF, DP-EqF, and SD-EqF are good candidates for high performance INS filter design with the TG-EqF demonstrating superior performance.

9 Acknowledgment

The authors would like to thank Martin Scheiber for his invaluable support and insightful discussions, which helped achieve the results presented in the manuscript. The authors would also like to thank the reviewers for their insightful critique that has substantially improved the contribution of the paper.

A Mathematical Preliminaries

In this section, we provide a quick overview of fundamental concepts in Lie theory.

A.1 Lie theory

A Lie group \mathbf{G} is a smooth manifold endowed with a smooth group structure. For any $X, Y \in \mathbf{G}$, the group multiplication is denoted XY , the group inverse X^{-1} and the identity element I .

Given a Lie group \mathbf{G} , \mathcal{G} denotes the \mathbf{G} -Torsor [19], which is defined as the set of elements of \mathbf{G} (the underlying manifold), but without the group structure.

For a given Lie group \mathbf{G} , the Lie algebra \mathfrak{g} can be modelled as a vector space corresponding to the tangent space at the identity of the group, together with a bilinear non-associative map $[\cdot, \cdot] : \mathfrak{g} \rightarrow \mathfrak{g}$ called the *Lie bracket*. For a matrix Lie group, the Lie bracket is equal to the matrix commutator:

$$[\eta, \kappa] = \eta\kappa - \kappa\eta,$$

for any $\eta, \kappa \in \mathfrak{g} \subset \mathbb{R}^{n \times n}$.

The Lie algebra \mathfrak{g} is isomorphic to a vector space \mathbb{R}^n of dimension $n = \dim(\mathfrak{g})$. Define the *wedge* map and its inverse, the *vee* map, as linear mappings between the vector space and the Lie algebra:

$$(\cdot)^\wedge : \mathbb{R}^n \rightarrow \mathfrak{g}, \quad (\cdot)^\vee : \mathfrak{g} \rightarrow \mathbb{R}^n.$$

For any $X, Y \in \mathbf{G}$, define the left and right translation

$$\begin{aligned} L_X : \mathbf{G} &\rightarrow \mathbf{G}, & L_X(Y) &= XY, \\ R_X : \mathbf{G} &\rightarrow \mathbf{G}, & R_X(Y) &= YX. \end{aligned}$$

The Adjoint map for the group \mathbf{G} , $\text{Ad}_X : \mathfrak{g} \rightarrow \mathfrak{g}$ is defined by

$$\text{Ad}_X [\mathbf{u}^\wedge] = \text{dL}_X \text{dR}_{X^{-1}} [\mathbf{u}^\wedge],$$

for every $X \in \mathbf{G}$ and $\mathbf{u}^\wedge \in \mathfrak{g}$, where dL_X , and dR_X denote the differentials of the left, and right translation, respectively. Given particular wedge and vee maps for a matrix Lie group, the Adjoint matrix is defined as the map $\text{Ad}_X^\vee : \mathbb{R}^n \rightarrow \mathbb{R}^n$

$$\text{Ad}_X^\vee \mathbf{u} = (\text{Ad}_X [\mathbf{u}^\wedge])^\vee.$$

In addition to the Adjoint map for the group \mathbf{G} , the adjoint map for the Lie algebra \mathfrak{g} can be defined as the differential at the identity of the Adjoint map for the group \mathbf{G} . The adjoint map for the Lie algebra $\text{ad}_{\mathbf{u}^\wedge} : \mathfrak{g} \rightarrow \mathfrak{g}$ is given by

$$\text{ad}_{\mathbf{u}^\wedge} [\mathbf{v}^\wedge] = [\mathbf{u}^\wedge, \mathbf{v}^\wedge],$$

and is equivalent to the Lie bracket. Given particular wedge and vee maps for a matrix Lie group, we define the adjoint matrix $\text{ad}_\mathbf{u}^\vee : \mathbb{R}^n \rightarrow \mathbb{R}^n$ to be

$$\text{ad}_\mathbf{u}^\vee \mathbf{v} = (\mathbf{u}^\wedge \mathbf{v}^\wedge - \mathbf{v}^\wedge \mathbf{u}^\wedge)^\vee = [\mathbf{u}^\wedge, \mathbf{v}^\wedge]^\vee.$$

For all $\mathbf{u}, \mathbf{v} \in \mathbb{R}^n$ and $X \in \mathbf{G}$, the two adjoints commute:

$$\begin{aligned} \text{Ad}_X [\text{ad}_{\mathbf{u}^\wedge} [\mathbf{v}^\wedge]] &= \text{ad}_{(\text{Ad}_X [\mathbf{u}^\wedge])} [\text{Ad}_X [\mathbf{v}^\wedge]], \\ \text{Ad}_X^\vee \text{ad}_\mathbf{u}^\vee \mathbf{v} &= \text{ad}_{\text{Ad}_X^\vee \mathbf{u}}^\vee \text{Ad}_X^\vee \mathbf{v}, \end{aligned}$$

A.2 Semi-direct product groups

A semi-direct product group $\mathbf{G} \ltimes \mathbf{H}$ can be seen as a generalization of the direct product group $\mathbf{G} \times \mathbf{H}$ where the underlying set is given by the cartesian product of two groups \mathbf{G} and \mathbf{H} . Contrary to the direct product, in the semi-direct product, the group multiplication is defined with the group \mathbf{G} that acts on a group \mathbf{H} by a group automorphism. Note that the semi-direct product group $\mathbf{G} \ltimes \mathbf{H}$ with the trivial automorphism corresponds to the direct product group $\mathbf{G} \times \mathbf{H}$.

In this work we will consider a semi-direct product symmetry group [23], [21], [22] $\mathbf{G}_\mathfrak{g}^\times := \mathbf{G} \ltimes \mathfrak{g}$ where \mathfrak{g} is the Lie algebra of \mathbf{G} , or a subalgebra of \mathbf{G} , that is, a vector space group under addition. Let $A, B \in \mathbf{G}$ and $a, b \in \mathfrak{g}$ and define $X = (A, a)$ and $Y = (B, b)$ elements of the symmetry group $\mathbf{G}_\mathfrak{g}^\times$. Group multiplication is defined to be the semi-direct product $YX = (BA, b + \text{Ad}_B[a])$. The inverse element is $X^{-1} = (A^{-1}, -\text{Ad}_{A^{-1}}[a])$ and identity element is $(I, 0)$.

A.3 Lie group action and homogeneous space

A right group action of a Lie group \mathbf{G} on a differentiable manifold \mathcal{M} is a smooth map $\phi : \mathbf{G} \times \mathcal{M} \rightarrow \mathcal{M}$ that satisfies

$$\phi(I, \xi) = \xi, \quad \phi(X, \phi(Y, \xi)) = \phi(YX, \xi),$$

for any $X, Y \in \mathbf{G}$ and $\xi \in \mathcal{M}$. A right group action ϕ induces a family of diffeomorphism $\phi_X : \mathcal{M} \rightarrow \mathcal{M}$ and smooth projections $\phi_\xi : \mathbf{G} \rightarrow \mathcal{M}$. The group action ϕ is said to be transitive if the induced projection ϕ_ξ is surjective. In this case, \mathcal{M} is a homogeneous space of \mathbf{G} .

A.4 Important Lie groups

The *special orthogonal group* $\mathbf{SO}(3)$ is the Lie group of 3D rotations in space. The special orthogonal group and its Lie algebra are defined as follows:

$$\begin{aligned} \mathbf{SO}(3) &= \left\{ \mathbf{A} \in \mathbb{R}^{3 \times 3} \mid \mathbf{A}\mathbf{A}^\top = \mathbf{I}_3, \det(\mathbf{A}) = 1 \right\}, \\ \mathfrak{so}(3) &= \left\{ \boldsymbol{\omega}^\wedge \in \mathbb{R}^{3 \times 3} \mid \boldsymbol{\omega}^\wedge = -\boldsymbol{\omega}^{\wedge\top}, \boldsymbol{\omega}^\wedge \mathbf{v} = \boldsymbol{\omega} \times \mathbf{v} \right\}, \end{aligned}$$

where \times represents the cross-product.

The *special Euclidean group* $\mathbf{SE}(3)$ is the group of 3D rigid body transformation in space. Note that $\mathbf{SE}(3)$ is defined as a semi-direct product group, specifically, $\mathbf{SE}(3) := \mathbf{SO}(3) \ltimes \mathbb{R}^3$. The special Euclidean group and its Lie algebra are defined as follows:

$$\begin{aligned} \mathbf{SE}(3) &= \left\{ \begin{bmatrix} \mathbf{A} & \mathbf{b} \\ \mathbf{0}_{1 \times 3} & 1 \end{bmatrix} \in \mathbb{R}^{4 \times 4} \mid \mathbf{A} \in \mathbf{SO}(3), \mathbf{b} \in \mathbb{R}^3 \right\}, \\ \mathfrak{se}(3) &= \left\{ \begin{bmatrix} \boldsymbol{\omega}^\wedge & \mathbf{w} \\ \mathbf{0}_{1 \times 3} & 0 \end{bmatrix} \in \mathbb{R}^{4 \times 4} \mid \boldsymbol{\omega}^\wedge \in \mathfrak{so}(3), \mathbf{w} \in \mathbb{R}^3 \right\}, \end{aligned}$$

The *extended special Euclidean group* $\mathbf{SE}_2(3)$ [2, 1, 3, 6] is an extension of the special Euclidean group. The group and its Lie algebra are defined as follows:

$$\begin{aligned} \mathbf{SE}_2(3) &= \left\{ \begin{bmatrix} \mathbf{A} & \mathbf{a} & \mathbf{b} \\ \mathbf{0}_{1 \times 3} & 1 & 0 \\ \mathbf{0}_{1 \times 3} & 0 & 1 \end{bmatrix} \in \mathbb{R}^{5 \times 5} \mid \mathbf{A} \in \mathbf{SO}(3), \mathbf{a}, \mathbf{b} \in \mathbb{R}^3 \right\}, \\ \mathfrak{se}_2(3) &= \left\{ \begin{bmatrix} \boldsymbol{\omega}^\wedge & \mathbf{v} & \mathbf{w} \\ \mathbf{0}_{1 \times 3} & 0 & 0 \\ \mathbf{0}_{1 \times 3} & 0 & 0 \end{bmatrix} \in \mathbb{R}^{5 \times 5} \mid \boldsymbol{\omega}^\wedge \in \mathfrak{so}(3), \mathbf{v}, \mathbf{w} \in \mathbb{R}^3 \right\}. \end{aligned}$$

The *homogenous Galilean group* $\mathbf{HG}(3)$ is the group of 3D rotation and relative velocity transformations.

$\mathbf{HG}(3)$ is isomorphic with $\mathbf{SE}(3)$ but acts on physical velocities rather than physical translations. The homogeneous Galilean group and its Lie algebra are defined as follows:

$$\mathbf{HG}(3) = \left\{ \begin{bmatrix} \mathbf{A} & \mathbf{a} \\ \mathbf{0}_{1 \times 3} & 1 \end{bmatrix} \in \mathbb{R}^{4 \times 4} \mid \mathbf{A} \in \mathbf{SO}(3), \mathbf{a} \in \mathbb{R}^3 \right\},$$

$$\mathfrak{hg}(3) = \left\{ \begin{bmatrix} \boldsymbol{\omega}^\wedge & \mathbf{v} \\ \mathbf{0}_{1 \times 3} & 0 \end{bmatrix} \in \mathbb{R}^{4 \times 4} \mid \boldsymbol{\omega}^\wedge \in \mathfrak{so}(3), \mathbf{v} \in \mathbb{R}^3 \right\},$$

B Linearization Error and Equivariant Filter Design with Different Symmetries

In this section, we explicitly derive the linearization error in the error dynamics and the related filter matrices of each filter presented in Tab. 2.

B.1 Logarithm map of semi-direct product group

As mentioned in Sec. 6, for the semi-direct product groups $\mathbf{G} \ltimes \mathfrak{g}$ where \mathfrak{g} is the Lie algebra of \mathbf{G} , we will use a matrix realization to compute the exponential algebraically. Define $X = (C, \gamma) \in \mathbf{G} \ltimes \mathfrak{g}$, then X has a matrix representation given by

$$X = \begin{bmatrix} \text{Ad}_C^\vee & \vdots & \gamma^\vee \\ \dots & \dots & \dots \\ \mathbf{0} & \vdots & 1 \end{bmatrix} \in \mathbb{R}^{(\dim \mathfrak{g} + 1) \times (\dim \mathfrak{g} + 1)}$$

The logarithm is then given by

$$\log_{\mathbf{G} \ltimes \mathfrak{g}}(X) = \begin{bmatrix} \text{ad}_{\log_{\mathbf{G}}(C)}^\vee & \vdots & J_l(\log_{\mathbf{G}}(C))^{-1} \gamma^\vee \\ \dots & \dots & \dots \\ \mathbf{0} & \vdots & 0 \end{bmatrix},$$

where $J_l(\log_{\mathbf{G}}(C))$ is the left Jacobian of $\log_{\mathbf{G}}(C)$,

$$J_l(\log_{\mathbf{G}}(C)) = \sum_{k=0}^{\infty} \frac{1}{(k+1)!} \text{ad}_{\log_{\mathbf{G}}(C)}^\vee{}^k.$$

B.2 MEKF linearization error and filter design

B.2.1 Overview

The state space is defined to be $\mathcal{M} := \mathbf{SO}(3) \times \mathbb{R}^3 \times \mathbb{R}^3 \times \mathbb{R}^3 \times \mathbb{R}^3$ with $\xi := (\mathbf{R}, \mathbf{v}, \mathbf{p}, \mathbf{b}_\omega, \mathbf{b}_a) \in \mathcal{M}$. Choose the origin to be $\xi := (\mathbf{I}_3, \mathbf{0}_{3 \times 1}, \mathbf{0}_{3 \times 1}, \mathbf{0}_{3 \times 1}, \mathbf{0}_{3 \times 1}) \in \mathcal{M}$. The velocity input is given by $u := (\boldsymbol{\omega}, \mathbf{a}, \boldsymbol{\tau}_\omega, \boldsymbol{\tau}_a)$.

The symmetry group of MEKF is given by $\mathbf{G}_O := \mathbf{SO}(3) \times \mathbb{R}^{12}$. Define the filter state $\hat{X} = (\hat{A}, \hat{a}, \hat{b}, \hat{\alpha}, \hat{\beta}) \in \mathbf{G}_O$, where $\hat{A} \in \mathbf{SO}(3)$ and $\hat{a}, \hat{b}, \hat{\alpha}, \hat{\beta} \in \mathbb{R}^3$. The state estimate is given by

$$\hat{\xi} := \phi(\hat{X}, \hat{\xi}) = (\hat{A}, \hat{a}, \hat{b}, \hat{\alpha}, \hat{\beta}) = (\hat{\mathbf{R}}, \hat{\mathbf{v}}, \hat{\mathbf{p}}, \hat{\mathbf{b}}_\omega, \hat{\mathbf{b}}_a). \quad (\text{B.1})$$

The state error is defined as

$$e := \phi(\hat{X}^{-1}, \xi) = (\mathbf{R} \hat{A}^\top, \mathbf{v} - \hat{a}, \mathbf{p} - \hat{b}, \mathbf{b}_\omega - \hat{\alpha}, \mathbf{b}_a - \hat{\beta}),$$

$$= (\mathbf{R} \hat{\mathbf{R}}^\top, \mathbf{v} - \hat{\mathbf{v}}, \mathbf{p} - \hat{\mathbf{p}}, \mathbf{b}_\omega - \hat{\mathbf{b}}_\omega, \mathbf{b}_a - \hat{\mathbf{b}}_a). \quad (\text{B.2})$$

B.2.2 Error dynamics

The error dynamics related to Equ. (B.2) for each state is given by

$$\begin{aligned} \dot{e}_R &= \frac{d}{dt}(\mathbf{R} \hat{\mathbf{R}}^\top) \\ &= \mathbf{R}(\boldsymbol{\omega} - \mathbf{b}_\omega)^\wedge \hat{\mathbf{R}}^\top - \mathbf{R} \hat{\mathbf{R}}^\top \hat{\mathbf{R}}(\boldsymbol{\omega} - \hat{\mathbf{b}}_\omega)^\wedge \hat{\mathbf{R}}^\top \\ &= \mathbf{R}(\boldsymbol{\omega} - \mathbf{b}_\omega - \boldsymbol{\omega} + \hat{\mathbf{b}}_\omega)^\wedge \hat{\mathbf{R}}^\top \\ &= -e_R \hat{\mathbf{R}} e_{b_\omega}^\wedge \hat{\mathbf{R}}^\top \\ &= -e_R (\hat{\mathbf{R}} e_{b_\omega})^\wedge; \\ \dot{e}_v &= \frac{d}{dt}(\mathbf{v} - \hat{\mathbf{v}}) = \dot{\mathbf{v}} - \dot{\hat{\mathbf{v}}} \\ &= \mathbf{R}(\mathbf{a} - \mathbf{b}_a)^\wedge + \mathbf{g} - \hat{\mathbf{R}}(\mathbf{a} - \hat{\mathbf{b}}_a)^\wedge - \mathbf{g} \\ &= \mathbf{R}(\mathbf{a} - \mathbf{b}_a)^\wedge - \hat{\mathbf{R}}(\mathbf{a} - \hat{\mathbf{b}}_a)^\wedge \\ &= e_R \hat{\mathbf{R}}(\mathbf{a} - \mathbf{b}_a) - \hat{\mathbf{R}}(\mathbf{a} - \hat{\mathbf{b}}_a); \\ \dot{e}_p &= \frac{d}{dt}(\mathbf{p} - \hat{\mathbf{p}}) = \dot{\mathbf{p}} - \dot{\hat{\mathbf{p}}} \\ &= \mathbf{v} - \hat{\mathbf{v}} = e_v; \\ \dot{e}_b &= \frac{d}{dt}(\mathbf{b} - \hat{\mathbf{b}}) = \mathbf{0}. \end{aligned}$$

The local coordinate chart $\varepsilon = \log_{\mathbf{G}_O} \circ \phi_\xi^{-1}(e)$ for each state is given by

$$\varepsilon_R := \log_{\mathbf{SO}(3)}(e_R)^\vee \in \mathbb{R}^3$$

$$\varepsilon_{v,p,b_\omega,b_a} := e_{v,p,b_\omega,b_a} \in \mathbb{R}^3.$$

The linearization of $\dot{e}_R = \text{D exp}(\varepsilon_R^\wedge)[\dot{\varepsilon}_R^\wedge]$ is given by

$$\begin{aligned} e_R \frac{\text{I} - \exp(-\text{ad}_{\varepsilon_R^\wedge})}{\text{ad}_{\varepsilon_R^\wedge}} \dot{\varepsilon}_R^\wedge &= -e_R (\hat{\mathbf{R}} e_{b_\omega})^\wedge \\ (\text{I} + \mathcal{O}(\varepsilon_R^\wedge)) \dot{\varepsilon}_R^\wedge &= (\hat{\mathbf{R}} e_{b_\omega})^\wedge \\ \dot{\varepsilon}_R &= \hat{\mathbf{R}} e_{b_\omega} + \mathcal{O}(\varepsilon_R^2). \end{aligned}$$

The linearization of $\dot{e}_v = \dot{\varepsilon}_v$ is given by

$$\begin{aligned}\dot{e}_v &= e_R \hat{\mathbf{R}}(\mathbf{a} - \mathbf{b}_a) - \hat{\mathbf{R}}(\mathbf{a} - \hat{\mathbf{b}}_a) \\ &= (\mathbf{I} + \varepsilon_R^\wedge + O(\varepsilon_R^2)) \hat{\mathbf{R}}(\mathbf{a} - \mathbf{b}_a) - \hat{\mathbf{R}}(\mathbf{a} - \hat{\mathbf{b}}_a) \\ &= \hat{\mathbf{R}}(\hat{\mathbf{b}}_a - \mathbf{b}_a) + \varepsilon_R^\wedge \hat{\mathbf{R}}(\mathbf{a} - \mathbf{b}_a) + O(\varepsilon_R^2) \\ &= -\hat{\mathbf{R}}\varepsilon_{b_a} + \varepsilon_R^\wedge \hat{\mathbf{R}}(\mathbf{a} - \varepsilon_{b_a} - \hat{\mathbf{b}}_a) + O(\varepsilon^2) \\ &= -\hat{\mathbf{R}}\varepsilon_{b_a} + \varepsilon_R^\wedge \hat{\mathbf{R}}(\mathbf{a} - \hat{\mathbf{b}}_a) - \varepsilon_R^\wedge \hat{\mathbf{R}}\varepsilon_{b_a} + O(\varepsilon_R^2) \\ &= -(\hat{\mathbf{R}}(\mathbf{a} - \hat{\mathbf{b}}_a))^\wedge \varepsilon_R - \hat{\mathbf{R}}\varepsilon_{b_a} + O(\varepsilon^2).\end{aligned}$$

The linearization of $\dot{e}_p = \dot{\varepsilon}_p$ is given by

$$\dot{\varepsilon}_p = \varepsilon_v.$$

The linearization of $\dot{e}_b = \dot{\varepsilon}_b$ is given by $\dot{\varepsilon}_b = \mathbf{0}$.

B.2.3 Filter design

From the linearization error analysis, it is trivial to see that the linearized error state matrix $\mathbf{A}_t^0 \mid \dot{\varepsilon} \simeq \mathbf{A}_t^0 \varepsilon$ is written

$$\mathbf{A}_t^0 = \begin{bmatrix} \vdots & -\hat{\mathbf{R}} & \mathbf{0}_{3 \times 3} \\ \mathbf{1} \mathbf{A} & \mathbf{0}_{3 \times 3} & -\hat{\mathbf{R}} \\ \vdots & \mathbf{0}_{3 \times 3} & \mathbf{0}_{3 \times 3} \\ \vdots & \vdots & \vdots \\ \mathbf{0}_{6 \times 9} & \mathbf{0}_{6 \times 6} & \vdots \end{bmatrix} \in \mathbb{R}^{15 \times 15}, \quad (\text{B.3})$$

where

$$\mathbf{1} \mathbf{A} = \begin{bmatrix} \mathbf{0}_{3 \times 3} & \mathbf{0}_{3 \times 3} & \mathbf{0}_{3 \times 3} \\ -(\hat{\mathbf{R}}(\mathbf{a} - \hat{\mathbf{b}}_a))^\wedge & \mathbf{0}_{3 \times 3} & \mathbf{0}_{3 \times 3} \\ \mathbf{0}_{3 \times 3} & \mathbf{I}_3 & \mathbf{0}_{3 \times 3} \end{bmatrix} \in \mathbb{R}^{9 \times 9}.$$

Position measurements are linear with respect to the defined error; therefore, the output matrix \mathbf{C}^0 yields

$$\mathbf{C}^0 = [\mathbf{0}_{3 \times 6} \quad \mathbf{I}_3 \quad \mathbf{0}_{3 \times 6}] \in \mathbb{R}^{3 \times 15}. \quad (\text{B.4})$$

It is straightforward to verify that the derived equivariant filter is equivalent to the well-known MEKF, and the EqF state matrix in Equ. (B.3) corresponds directly to the state matrix of the MEKF [26, Sec. 7]

B.3 Imperfect-IEKF

B.3.1 Overview

The state space is defined as $\mathcal{M} := \mathcal{SE}_2(3) \times \mathbb{R}^6$ with $\xi := (\mathbf{T}, \mathbf{b}) \in \mathcal{M}$. One has $\mathbf{T} = (\mathbf{R}, \mathbf{v}, \mathbf{p}) \in \mathcal{SE}_2(3)$

and $\mathbf{b} = (\mathbf{b}_\omega, \mathbf{b}_a) \in \mathbb{R}^6$. Choose the origin to be $\dot{\xi} = (\mathbf{I}_5, \mathbf{0}_{6 \times 1}) \in \mathcal{M}$. The velocity input is given by $u := (\boldsymbol{\omega}, \mathbf{a}, \boldsymbol{\tau}_\omega, \boldsymbol{\tau}_a)$.

The symmetry group of Imperfect-IEKF is given by $\mathbf{G}_{\text{ES}} : \mathbf{SE}_2(3) \times \mathbb{R}^6$. Define the filter state $\hat{X} = (\hat{C}, \hat{\gamma}) \in \mathbf{G}_{\text{ES}}$ with $\hat{C} = (\hat{A}, \hat{a}, \hat{b}) \in \mathbf{SE}_2(3)$ and $\hat{\gamma} = (\hat{\gamma}_\omega, \hat{\gamma}_a) \in \mathbb{R}^6$. The state estimate is given by

$$\hat{\xi} := \phi(\hat{X}, \hat{\xi}) = (\hat{A}, \hat{\gamma}) = (\hat{\mathbf{T}}, \hat{\mathbf{b}}). \quad (\text{B.5})$$

The state error is defined as

$$\begin{aligned}e &:= \phi(\hat{X}^{-1}, \xi) = (\mathbf{T} \hat{C}^{-1}, \mathbf{b} - \hat{\gamma}), \\ &= (\mathbf{T} \hat{\mathbf{T}}^{-1}, \mathbf{b} - \hat{\mathbf{b}}).\end{aligned} \quad (\text{B.6})$$

B.3.2 Error dynamics

The error dynamics related to Equ. (B.6) for each state is given by

$$\begin{aligned}\dot{e}_R &= -e_R(\hat{\mathbf{R}}e_{b_\omega})^\wedge \quad (\text{Derivation same as MEKF}); \\ \dot{e}_v &= \frac{d}{dt}(-\mathbf{R} \hat{\mathbf{R}}^\top + \mathbf{v}) = \frac{d}{dt}(-\mathbf{R} \hat{\mathbf{R}}^\top \hat{\mathbf{v}} + \mathbf{v}) \\ &= -\dot{e}_R \hat{\mathbf{v}} - e_R \dot{\hat{\mathbf{v}}} + \dot{\mathbf{v}} \\ &= e_R(\hat{\mathbf{R}}e_{b_\omega})^\wedge \hat{\mathbf{v}} - e_R \hat{\mathbf{R}}(\mathbf{a} - \hat{\mathbf{b}}_a) - e_R \mathbf{g} + \mathbf{R}(\mathbf{a} - \mathbf{b}_a) + \mathbf{g} \\ &= e_R(\hat{\mathbf{R}}e_{b_\omega})^\wedge \hat{\mathbf{v}} - e_R \hat{\mathbf{R}}(\mathbf{a} - \hat{\mathbf{b}}_a) - e_R \mathbf{g} \\ &\quad + e_R \hat{\mathbf{R}}(\mathbf{a} - e_{b_a} + \hat{\mathbf{b}}_a) + \mathbf{g}; \\ \dot{e}_p &= \frac{d}{dt}(-\mathbf{R} \hat{\mathbf{R}}^\top \hat{\mathbf{p}} + \mathbf{p}) \\ &= -\dot{e}_R \hat{\mathbf{p}} - e_R \dot{\hat{\mathbf{p}}} + \dot{\mathbf{p}} \\ &= e_R(\hat{\mathbf{R}}e_{b_\omega})^\wedge \hat{\mathbf{p}} - e_R \hat{\mathbf{v}} + \mathbf{v} \\ &= e_R(\hat{\mathbf{R}}e_{b_\omega})^\wedge \hat{\mathbf{p}} + e_v; \\ \dot{e}_b &= \mathbf{0}.\end{aligned}$$

The local coordinate chart $\varepsilon = \log_{\mathbf{G}_{\text{ES}}} \circ \phi_\xi^{-1}(e)$ for each state is given by

$$\begin{aligned}\varepsilon_T &:= \log_{\mathbf{SE}_2(3)}(\phi_\xi^{-1}(e_T))^\vee = \log_{\mathbf{SE}_2(3)}(e_T)^\vee \in \mathbb{R}^9 \\ \varepsilon_{b_\omega, b_a} &:= e_{b_\omega, b_a} \in \mathbb{R}^3.\end{aligned}$$

The linearization of \dot{e}_R is the same as the derivation in MEKF, given by

$$\dot{e}_R = \hat{\mathbf{R}}\varepsilon_{b_\omega} + O(\varepsilon_R^2).$$

The linearization of $\dot{e}_v = \dot{\varepsilon}_v + \mathcal{O}(\varepsilon^2)$ is given by

$$\begin{aligned}\dot{e}_v &= -(\mathbf{I} + \varepsilon_R^\wedge + \mathcal{O}(\varepsilon_R^2))(\hat{\mathbf{R}}\varepsilon_{b_\omega})^\wedge \hat{\mathbf{v}} \\ &\quad - (\mathbf{I} + \varepsilon_R^\wedge + \mathcal{O}(\varepsilon_R^2)) \hat{\mathbf{R}}(\mathbf{a} - \hat{\mathbf{b}}_a) \\ &\quad - (\mathbf{I} + \varepsilon_R^\wedge + \mathcal{O}(\varepsilon_R^2)) \mathbf{g} \\ &\quad + (\mathbf{I} + \varepsilon_R^\wedge + \mathcal{O}(\varepsilon_R^2)) \hat{\mathbf{R}}(\mathbf{a} - \varepsilon_{b_a} + \hat{\mathbf{b}}_a) \\ &\quad + \mathbf{g} + \mathcal{O}(\varepsilon^2) \\ &= -\hat{\mathbf{v}}^\wedge \hat{\mathbf{R}}\varepsilon_{b_\omega} - \hat{\mathbf{R}}\varepsilon_{b_a} + \mathbf{g}^\wedge \varepsilon_R + \mathcal{O}(\varepsilon^2).\end{aligned}$$

The linearization of $\dot{e}_p = \dot{\varepsilon}_p + \mathcal{O}(\varepsilon^2)$ is given by

$$\begin{aligned}\dot{e}_p &= (\mathbf{I} + \varepsilon_R^\wedge + \mathcal{O}(\varepsilon_R^2))(\hat{\mathbf{R}}\varepsilon_{b_\omega})^\wedge \hat{\mathbf{p}} + \varepsilon_v + \mathcal{O}(\varepsilon^2) \\ &= \varepsilon_v - \hat{\mathbf{p}}^\wedge \varepsilon_{b_\omega} + \mathcal{O}(\varepsilon^2).\end{aligned}$$

The linearization of $\dot{e}_b = \dot{\varepsilon}_b$ is given by $\dot{e}_b = \mathbf{0}$.

B.3.3 Filter design

The linearized error state matrix $\mathbf{A}_t^0 \mid \dot{\varepsilon} \simeq \mathbf{A}_t^0 \varepsilon$ yields

$$\mathbf{A}_t^0 = \begin{bmatrix} \vdots & -\hat{\mathbf{R}} & \mathbf{0}_{3 \times 3} \\ {}_2\mathbf{A} & -\hat{\mathbf{v}}^\wedge \hat{\mathbf{R}} & -\hat{\mathbf{R}} \\ \vdots & -\hat{\mathbf{p}}^\wedge \hat{\mathbf{R}} & \mathbf{0}_{3 \times 3} \\ \vdots & \vdots & \vdots \\ \mathbf{0}_{6 \times 9} & \mathbf{0}_{6 \times 6} & \vdots \end{bmatrix} \in \mathbb{R}^{15 \times 15}, \quad (\text{B.7})$$

where

$${}_2\mathbf{A} = \begin{bmatrix} \mathbf{0}_{3 \times 3} & \mathbf{0}_{3 \times 3} & \mathbf{0}_{3 \times 3} \\ \mathbf{g}^\wedge & \mathbf{0}_{3 \times 3} & \mathbf{0}_{3 \times 3} \\ \mathbf{0}_{3 \times 3} & \mathbf{I}_3 & \mathbf{0}_{3 \times 3} \end{bmatrix} \in \mathbb{R}^{9 \times 9} \quad (\text{B.8})$$

Position measurements formulated according to Equ. (34) are equivariant, yielding the following output matrix

$$\mathbf{C}^* = \left[\frac{1}{2} (y + \hat{\mathbf{p}})^\wedge \mathbf{0}_{3 \times 3} \quad -\mathbf{I}_3 \quad \mathbf{0}_{3 \times 6} \right] \in \mathbb{R}^{3 \times 15}. \quad (\text{B.9})$$

It is trivial to verify that the state matrix in Equ. (B.7), derived according to equivariant filter design principles, directly corresponds to the state matrix in the Imperfect-IEKF [13, Sec. 7].

B.4 TG-EqF

B.4.1 Overview

The state space is defined as $\mathcal{M} := \mathcal{SE}_2(3) \times \mathbb{R}^9$ with $\xi := (\mathbf{T}, \hat{\mathbf{b}}) \in \mathcal{M}$. One has $\mathbf{T} = (\mathbf{R}, \mathbf{v}, \mathbf{p}) \in \mathcal{SE}_2(3)$ and $\hat{\mathbf{b}} = (\hat{\mathbf{b}}_\omega, \hat{\mathbf{b}}_a, \hat{\mathbf{b}}_\nu) \in \mathbb{R}^9$. Choose the origin to be

$\hat{\xi} = (\mathbf{I}_5, \mathbf{0}_{9 \times 1}) \in \mathcal{M}$. The velocity input is given by $u := (\boldsymbol{\omega}, \mathbf{a}, \boldsymbol{\nu}, \boldsymbol{\tau}_\omega, \boldsymbol{\tau}_a, \boldsymbol{\tau}_\nu)$.

The symmetry group of TG-EqF is given by $\mathbf{G}_{\mathbf{TG}} : \mathbf{SE}_2(3) \ltimes \mathfrak{se}_2(3)$. Define the filter state $\hat{X} = (\hat{C}, \hat{\gamma}) \in \mathbf{G}_{\mathbf{TG}}$ with $\hat{C} = (\hat{A}, \hat{a}, \hat{b}) \in \mathbf{SE}_2(3)$ and $\hat{\gamma} = (\hat{\gamma}_\omega, \hat{\gamma}_a, \hat{\gamma}_\nu)^\wedge \in \mathfrak{se}_2(3)$. The state estimate is given by

$$\hat{\xi} := \phi(\hat{X}, \hat{\xi}) = (\hat{C}, \text{Ad}_{\hat{C}^{-1}}(-\hat{\gamma}^\vee)) = (\hat{\mathbf{T}}, \hat{\mathbf{b}}). \quad (\text{B.10})$$

The state error is defined as

$$e := \phi(\hat{X}^{-1}, \xi) = (\mathbf{T}\hat{C}^{-1}, \mathbf{Ad}_{\hat{C}}^\vee(\mathbf{b} + \text{Ad}_{\hat{C}^{-1}}[\hat{\gamma}]^\vee)) \quad (\text{B.11})$$

$$= (\mathbf{T}\hat{C}^{-1}, \mathbf{Ad}_{\hat{C}}^\vee \mathbf{b} + \hat{\gamma}^\vee) \quad (\text{B.12})$$

$$= (\mathbf{T} \hat{\mathbf{T}}^{-1}, \mathbf{Ad}_{\hat{\mathbf{T}}}^\vee(\mathbf{b} - \hat{\mathbf{b}})) \quad (\text{B.13})$$

B.4.2 Error dynamics

Navigation states The error dynamics related to Equ. (B.11) for the navigation states $e_T = \mathbf{T} \hat{\mathbf{T}}^{-1}$ is given by

$$\begin{aligned}\dot{e}_T &= \dot{\mathbf{T}} \hat{\mathbf{T}}^{-1} - \mathbf{T} \dot{\hat{\mathbf{T}}}^{-1} \hat{\mathbf{T}} \hat{\mathbf{T}}^{-1} \\ &= \mathbf{T}(\mathbf{W} - \mathbf{B} + \mathbf{N}) \hat{\mathbf{T}}^{-1} + (\mathbf{G} - \mathbf{N}) \mathbf{T} \hat{\mathbf{T}}^{-1} \\ &\quad - e_T \hat{\mathbf{T}}(\mathbf{W} - \hat{\mathbf{B}} + \mathbf{N}) \hat{\mathbf{T}}^{-1} - e_T(\mathbf{G} - \mathbf{N}) \hat{\mathbf{T}} \hat{\mathbf{T}}^{-1} \\ &= e_T \hat{\mathbf{T}}(\mathbf{W} - \mathbf{B} + \mathbf{N}) \hat{\mathbf{T}}^{-1} - e_T \hat{\mathbf{T}}(\mathbf{W} - \hat{\mathbf{B}} + \mathbf{N}) \hat{\mathbf{T}}^{-1} \\ &\quad + (\mathbf{G} - \mathbf{N})e_T - e_T(\mathbf{G} - \mathbf{N}) \\ &= e_T \text{Ad}_{\hat{\mathbf{T}}}[\hat{\mathbf{B}} - \mathbf{B}] + (\mathbf{G} - \mathbf{N})e_T - e_T(\mathbf{G} - \mathbf{N}).\end{aligned}$$

The above dynamics can be separate to two parts: $\dot{e}_T = \dot{e}_{T_W} + \dot{e}_{T_G}$, where $\dot{e}_{T_W} = e_T \text{Ad}_{\hat{\mathbf{T}}}[\hat{\mathbf{B}} - \mathbf{B}]$ and $\dot{e}_{T_G} = (\mathbf{G} - \mathbf{N})e_T - e_T(\mathbf{G} - \mathbf{N})$. The linearization can be derived separately for each part.

The local coordinate chart is given by $\varepsilon = \log \circ \phi_\xi^{-1}(e)$. For each state, one has

$$\begin{aligned}e_T &= \exp_{\mathbf{SE}_2(3)}(\varepsilon_T^\wedge), \\ e_b &= \text{Ad}_{e_T^{-1}}[(-J_l(\varepsilon_T)\varepsilon_b)^\wedge],\end{aligned}$$

where the exponential map $\exp_{\mathbf{SE}_2(3) \ltimes \mathfrak{se}_2(3)}$ is derived from the semi-direct product structure, and $J_l(\varepsilon_T)$ is the left Jacobian of $\mathbf{SE}_2(3)$, given by

$$J_l(\varepsilon_T) = \sum_{k=0}^{\infty} \frac{1}{(k+1)!} \text{ad}_{\varepsilon_T}^k.$$

Recall that by definition Equ. (B.11) one has $e_b^\wedge := \text{Ad}_{\hat{\mathbf{T}}}[(\mathbf{b} - \hat{\mathbf{b}})^\wedge]$ with $\mathbf{b}^\wedge = \mathbf{B}$, and $\hat{\mathbf{b}}^\wedge = \hat{\mathbf{B}}$. Hence,

for \dot{e}_{TW} one has

$$\dot{e}_{TW} = e_T \text{Ad}_{\hat{\mathbf{T}}} [\hat{\mathbf{B}} - \mathbf{B}] = -e_T e_b^\wedge.$$

Substituting the local coordinate yields

$$\begin{aligned} D \exp_{\mathbf{SE}_2(3)}(\varepsilon_T^\wedge) [\dot{e}_{TW}^\wedge] &= -e_T \text{Ad}_{e_T^{-1}} [(-J_l(\varepsilon_T) \varepsilon_b)^\wedge] \\ e_T \frac{I - \exp(-\text{ad}_{\varepsilon_T^\wedge})}{\text{ad}_{\varepsilon_T^\wedge}} \dot{e}_{TW}^\wedge &= -e_T \text{Ad}_{e_T^{-1}} [(-J_l(\varepsilon_T) \varepsilon_b)^\wedge] \\ \text{Ad}_{e_T} \frac{I - \exp(-\text{ad}_{\varepsilon_T^\wedge})}{\text{ad}_{\varepsilon_T^\wedge}} \dot{e}_{TW}^\wedge &= (J_l(\varepsilon_T) \varepsilon_b)^\wedge. \end{aligned} \quad (\text{B.14})$$

Because $\text{Ad}_{e_T} = \text{Ad}_{\exp(\varepsilon_T^\wedge)} = \exp(\text{ad}_{\varepsilon_T^\wedge})$, the term on the left side in Equ. (B.14) can be modified as

$$\begin{aligned} \text{Ad}_{e_T} \frac{I - \exp(-\text{ad}_{\varepsilon_T^\wedge})}{\text{ad}_{\varepsilon_T^\wedge}} &= \exp(\text{ad}_{\varepsilon_T^\wedge}) \frac{I - \exp(-\text{ad}_{\varepsilon_T^\wedge})}{\text{ad}_{\varepsilon_T^\wedge}} \\ &= \frac{\exp(\text{ad}_{\varepsilon_T^\wedge}) - I}{\text{ad}_{\varepsilon_T^\wedge}} \quad (\text{Expanding exp,}) \\ &= \sum_{k=0}^{\infty} \frac{1}{(k+1)!} \text{ad}_{\varepsilon_T^\wedge}^k = J_l(\varepsilon_T). \end{aligned} \quad (\text{B.15})$$

Hence, for the linearization of \dot{e}_{TW} , one has

$$\dot{e}_{TW} = \varepsilon_b.$$

For the second part $\dot{e}_{TG} = D \exp_{\mathbf{SE}_2(3)}(\varepsilon_T^\wedge) [\dot{e}_{TG}^\wedge]$, one has

$$e_T \frac{I - \exp(-\text{ad}_{\varepsilon_T^\wedge})}{\text{ad}_{\varepsilon_T^\wedge}} \dot{e}_{TG}^\wedge = \begin{bmatrix} \mathbf{0}_{3 \times 3} & \mathbf{g} - e_R \mathbf{g} & e_v \\ \mathbf{0}_{1 \times 3} & 0 & 0 \\ \mathbf{0}_{1 \times 3} & 0 & 0 \end{bmatrix}. \quad (\text{B.16})$$

Multiply both sides of Equ. (B.16) by e_T^{-1} and then apply Ad_{e_T} to both sides:

$$\begin{aligned} \text{Ad}_{e_T} \frac{I - \exp(-\text{ad}_{\varepsilon_T})}{\text{ad}_{\varepsilon_T}} \dot{e}_{TG} &= \text{Ad}_{e_T} e_T^{-1} \begin{bmatrix} \mathbf{0}_{3 \times 3} & \mathbf{g} - e_R \mathbf{g} & e_v \\ \mathbf{0}_{1 \times 3} & 0 & 0 \\ \mathbf{0}_{1 \times 3} & 0 & 0 \end{bmatrix} \\ &= \begin{bmatrix} \mathbf{0}_{3 \times 3} & \mathbf{g} - e_R \mathbf{g} & e_v \\ \mathbf{0}_{1 \times 3} & 0 & 0 \\ \mathbf{0}_{1 \times 3} & 0 & 0 \end{bmatrix}. \end{aligned}$$

Use the result from Equ. (B.15):

$$J_l(\varepsilon_T) \dot{e}_{TG} = \begin{bmatrix} \mathbf{0}_{3 \times 3} & (I - e_R) \mathbf{g} & J_l(\varepsilon_R) \varepsilon_v \\ \mathbf{0}_{1 \times 3} & 0 & 0 \\ \mathbf{0}_{1 \times 3} & 0 & 0 \end{bmatrix}. \quad (\text{B.17})$$

Note that:

$$\begin{aligned} I - e_R &= I - \exp(\varepsilon_R^\wedge) \\ &= I - \sum_{k=0}^{\infty} \frac{1}{k!} \varepsilon_R^{\wedge k} \\ &= -\left(\sum_{k=0}^{\infty} \frac{1}{(k+1)!} \varepsilon_R^{\wedge k} \right) \varepsilon_R^\wedge \\ &= -J_l(\varepsilon_R) \varepsilon_R^\wedge. \end{aligned}$$

One can then simplify Equ. (B.17) to

$$\dot{e}_{TG} = \begin{bmatrix} \mathbf{0}_{3 \times 3} & \mathbf{g}^\wedge \varepsilon_R & \varepsilon_v \\ \mathbf{0}_{1 \times 3} & 0 & 0 \\ \mathbf{0}_{1 \times 3} & 0 & 0 \end{bmatrix}.$$

Combining the results for \dot{e}_{TW} and \dot{e}_{TG} , one has

$$\dot{e}_T = (\varepsilon_{b_\omega}, \varepsilon_{b_a} + \mathbf{g}^\wedge \varepsilon_R, \varepsilon_{b_v} + \varepsilon_v)^\wedge.$$

Bias states The linearization of the bias error are derived from the formula given by

$$\begin{aligned} \dot{\varepsilon} &= \mathbf{A}_t^0 \varepsilon + \mathcal{O}(\varepsilon^2), \\ \mathbf{A}_t^0 &= D_e|_{\xi} \vartheta(e) D_E|_I \phi_{\xi}(E) D_e|_{\xi} \Lambda(e, u^\circ) D_e|_0 \vartheta^{-1}(\varepsilon). \end{aligned}$$

In this case, because we choose normal coordinates as the local coordinate chart, that is, $\vartheta := \log \circ \phi_{\xi}^{-1}$, we have

$$\dot{\varepsilon} = D_e|_{\xi} \Lambda(e, \hat{u}) D_E|_I \phi_{\xi}(E) [\varepsilon] + \mathcal{O}(\varepsilon^2).$$

Evaluating $D\phi_{\xi}$ at I with direction $[\varepsilon_T, \varepsilon_b]$ yields

$$D\phi_{\xi}(I) [\varepsilon_T, \varepsilon_b] = (\varepsilon_T^\wedge, -\varepsilon_b^\wedge).$$

Evaluating $D\Lambda_{\hat{u}}$ at $\hat{\xi}$ with direction $[\varepsilon_T^\wedge, -\varepsilon_b^\wedge]$ yields

$$\begin{aligned} D\Lambda_{\hat{u}}(\hat{\xi}) [\varepsilon_T^\wedge, -\varepsilon_b^\wedge] &= (\sim, \text{ad}_{-\varepsilon_b^\wedge} [\Lambda_1(\hat{\xi}, \hat{u})]) \\ &= (\sim, \mathbf{ad}_{(\hat{w}^\wedge + \mathbf{G})}^\vee \varepsilon_b). \end{aligned}$$

Hence the linearization of bias error is given by

$$\dot{\varepsilon}_b = \mathbf{ad}_{(\hat{w}^\wedge + \mathbf{G})}^\vee \varepsilon_b + \mathcal{O}(\varepsilon^2).$$

B.4.3 Filter design

The linearized error state matrix $\mathbf{A}_t^0 | \dot{\varepsilon} \simeq \mathbf{A}_t^0 \varepsilon$ is defined according to

$$\mathbf{A}_t^0 = \begin{bmatrix} {}_2\mathbf{A} & \vdots & \mathbf{I}_9 \\ \vdots & \ddots & \vdots \\ \mathbf{0}_{9 \times 9} & \vdots & \mathbf{ad}_{(\hat{\mathbf{w}}^\wedge + \mathbf{G})}^\vee \end{bmatrix} \in \mathbb{R}^{18 \times 18}, \quad (\text{B.18})$$

with ${}_2\mathbf{A}$ in Equ. (B.8).

Position measurements formulated according to Equ. (34) are equivariant, yielding the following output matrix

$$\mathbf{C}^* = \left[\frac{1}{2} (y + \hat{p})^\wedge \mathbf{0}_{3 \times 3} \quad -\mathbf{I}_3 \quad \mathbf{0}_{3 \times 9} \right] \in \mathbb{R}^{3 \times 18}. \quad (\text{B.19})$$

Moreover, an additional constraint can be imposed on the virtual bias \mathbf{b}_ν ; that is, an additional measurement in the form of $h(\xi) = \mathbf{b}_\nu = \mathbf{0} \in \mathbb{R}^3$ can be considered, leading to the following output matrix

$$\mathbf{C}^0 = \begin{bmatrix} \mathbf{0}_{3 \times 3} & \mathbf{0}_{3 \times 3} & \mathbf{0}_{3 \times 3} & -\hat{\mathbf{R}}^\top & \mathbf{0}_{3 \times 3} & \hat{\mathbf{R}}^\top & \hat{\mathbf{p}}^\wedge \end{bmatrix} \in \mathbb{R}^{3 \times 18}. \quad (\text{B.20})$$

Note that for a practical implementation of the presented EqF the virtual inputs $\boldsymbol{\nu}$ is set to zero.

It is worth noticing that the EqF built on the \mathbf{G}_{TG} symmetry group is the only filter with exact linearization of the navigation error dynamics.

B.5 DP-EqF

B.5.1 Overview

The state space is defined as $\mathcal{M} := \mathcal{HG}(3) \times \mathbb{R}^3 \times \mathbb{R}^6$ with $\xi := (\mathbf{T}, \mathbf{p}, \mathbf{b}) \in \mathcal{M}$. One has $\mathbf{T} = (\mathbf{R}, \mathbf{v}) \in \mathcal{HG}(3)$ and $\mathbf{b} = (\mathbf{b}_\omega, \mathbf{b}_a) \in \mathbb{R}^6$. Choose the origin to be $\hat{\xi} = (\mathbf{I}_4, \mathbf{0}_{6 \times 1}, \mathbf{0}_{3 \times 1}) \in \mathcal{M}$. The velocity input is given by $u := (\boldsymbol{\omega}, \mathbf{a}, \boldsymbol{\tau}_\omega, \boldsymbol{\tau}_a, \boldsymbol{\nu})$.

The symmetry group of DP-EqF is given by $\mathbf{G}_{\text{DP}} : \mathbf{HG}(3) \ltimes \mathfrak{hg}(3) \times \mathbb{R}^3$. Define the filter state $\hat{X} = (\hat{B}, \hat{\beta}, \hat{c}) \in \mathbf{G}_{\text{DP}}$ with $\hat{B} = (\hat{A}, \hat{a}) \in \mathbf{HG}(3)$ and $\hat{\beta} = (\hat{\beta}_\omega, \hat{\beta}_a)^\wedge \in \mathfrak{hg}(3)$. The state estimate is given by

$$\hat{\xi} := \phi(\hat{X}, \hat{\xi}) = (\hat{B}, \text{Ad}_{\hat{B}^{-1}}(-\hat{\beta}), \hat{c}) = (\hat{\mathbf{T}}, \hat{\mathbf{b}}, \hat{\mathbf{p}}). \quad (\text{B.21})$$

The state error is defined as

$$e := \phi(\hat{X}^{-1}, \xi) = (\mathbf{T} \hat{B}^{-1}, \mathbf{Ad}_{\hat{B}}^\vee \mathbf{b} + \hat{\beta}^\vee, \mathbf{p} - \hat{c}) \quad (\text{B.22})$$

$$= (\mathbf{T} \hat{\mathbf{T}}^{-1}, \mathbf{Ad}_{\hat{\mathbf{T}}}^\vee (\mathbf{b} - \hat{\mathbf{b}}), \mathbf{p} - \hat{\mathbf{p}}) \quad (\text{B.23})$$

B.5.2 Error dynamics

Navigation states Because of the semi-direct product structure related to the rotation and velocity states

and the corresponding bias states, the derivation of the error dynamics of the $\mathcal{HG}(3)$ part is similar to the one in TG-EqF. In this case, one has

$$\begin{aligned} \dot{\varepsilon}_R &= \varepsilon_{b_\omega}, \\ \dot{\varepsilon}_v &= \varepsilon_{b_a} + \mathbf{g}^\wedge \varepsilon_R. \end{aligned}$$

For the position error, one has

$$\begin{aligned} \dot{\varepsilon}_p &= \dot{e}_p = \dot{\mathbf{p}} - \dot{\hat{\mathbf{p}}} = \mathbf{R} \boldsymbol{\nu} + \mathbf{v} - \hat{\mathbf{R}} \boldsymbol{\nu} - \hat{\mathbf{v}} \\ &= e_v + e_R \hat{\mathbf{v}} - \hat{\mathbf{v}} + e_R \hat{\mathbf{R}} \boldsymbol{\nu} - \hat{\mathbf{R}} \boldsymbol{\nu} \\ &= J_l(\varepsilon_R) \varepsilon_v + (\mathbf{I} + \varepsilon_R^\wedge + \mathcal{O}(\varepsilon_R^2)) (\hat{\mathbf{R}} \boldsymbol{\nu} + \hat{\mathbf{v}}) - (\hat{\mathbf{R}} \boldsymbol{\nu} + \hat{\mathbf{v}}) \\ &= J_l(\varepsilon_R) \varepsilon_v + (\mathbf{I} + \varepsilon_R^\wedge + \mathcal{O}(\varepsilon_R^2)) \hat{\boldsymbol{\nu}} - \hat{\boldsymbol{\nu}} \\ &= \varepsilon_v - \hat{\boldsymbol{\nu}}^\wedge \varepsilon_R + \mathcal{O}(\varepsilon^2). \end{aligned}$$

Bias states The derivation of bias error dynamics is the same as TG-EqF:

$$\dot{\varepsilon}_b = \mathbf{ad}_{(\hat{\mathbf{w}}^\wedge + \mathbf{G})}^\vee \varepsilon_b + \mathcal{O}(\varepsilon^2).$$

B.5.3 Filter design

The linearized error state matrix $\mathbf{A}_t^0 \mid \dot{\varepsilon} \simeq \mathbf{A}_t^0 \varepsilon$ is defined according to

$$\mathbf{A}_t^0 = \begin{bmatrix} {}_3\mathbf{A} & \mathbf{I}_6 & \mathbf{0}_{6 \times 3} \\ \mathbf{0}_{6 \times 6} & \mathbf{ad}_{(\hat{\mathbf{w}}^\wedge + \mathbf{G})}^\vee & \mathbf{0}_{6 \times 3} \\ {}_4\mathbf{A} & \mathbf{0}_{3 \times 6} & \mathbf{0}_{3 \times 3} \end{bmatrix} \in \mathbb{R}^{15 \times 15}, \quad (\text{B.24})$$

where

$$\begin{aligned} {}_3\mathbf{A} &= \begin{bmatrix} \mathbf{0}_{3 \times 3} & \mathbf{0}_{3 \times 3} \\ \mathbf{g}^\wedge & \mathbf{0}_{3 \times 3} \end{bmatrix} \in \mathbb{R}^{6 \times 6} \\ {}_4\mathbf{A} &= \begin{bmatrix} -\hat{\boldsymbol{\nu}}^\wedge & \mathbf{I}_3 \end{bmatrix} \in \mathbb{R}^{3 \times 6}. \end{aligned}$$

Position measurements are linear; therefore, the output matrix is written

$$\mathbf{C}^0 = \begin{bmatrix} \mathbf{0}_{3 \times 3} & \mathbf{0}_{3 \times 3} & \mathbf{0}_{3 \times 6} & \mathbf{I}_3 \end{bmatrix} \in \mathbb{R}^{3 \times 15}. \quad (\text{B.25})$$

Similar to the previous filter, for a practical implementation of the presented EqF, the virtual input $\boldsymbol{\nu}$ is set to zero.

B.6 SD-EqF

B.6.1 Overview

The state space is defined as $\mathcal{M} := \mathcal{SE}_2(3) \times \mathbb{R}^6$ with $\xi := (\mathbf{T}, \mathbf{b}) \in \mathcal{M}$. One has $\mathbf{T} = (\mathbf{R}, \mathbf{v}, \mathbf{p}) \in \mathcal{SE}_2(3)$ and $\mathbf{b} = (\mathbf{b}_\omega, \mathbf{b}_a) \in \mathbb{R}^6$. Choose the origin to be $\hat{\xi} = (\mathbf{I}_5, \mathbf{0}_{6 \times 1}) \in \mathcal{M}$. The velocity input is given by $u := (\boldsymbol{\omega}, \mathbf{a}, \boldsymbol{\tau}_\omega, \boldsymbol{\tau}_a)$.

The symmetry group of SD-EqF is given by $\mathbf{G}_{\text{SD}} : \mathbf{SE}_2(3) \ltimes \mathfrak{se}(3)$. Define the filter state $\hat{X} = (\hat{C}, \hat{\gamma}) \in \mathbf{G}_{\text{SD}}$ with $\hat{C} = (\hat{A}, \hat{a}, \hat{b}) \in \mathbf{SE}_2(3)$ and $\hat{\gamma} = (\hat{\gamma}_\omega, \hat{\gamma}_a)^\wedge \in \mathfrak{se}(3)$. The $\mathbf{SE}_2(3)$ component in \hat{X} can also be expressed in $\hat{C} = (\hat{B}, \hat{b})$ where $\hat{B} = (\hat{A}, \hat{a}) \in \mathbf{HG}(3)$. The state estimate is given by

$$\hat{\xi} := \phi(\hat{X}, \hat{\xi}) = (\hat{C}, \text{Ad}_{\hat{B}^{-1}}(-\hat{\gamma}^\vee)) = (\hat{\mathbf{T}}, \hat{\mathbf{b}}). \quad (\text{B.26})$$

The state error is defined as

$$e := \phi(\hat{X}^{-1}, \xi) = (\mathbf{T}\hat{C}^{-1}, \text{Ad}_{\hat{B}}^\vee(\mathbf{b} + \text{Ad}_{\hat{B}^{-1}}[\hat{\gamma}]^\vee)) \quad (\text{B.27})$$

$$= (\mathbf{T}\hat{C}^{-1}, \text{Ad}_{\hat{B}}^\vee \mathbf{b} + \hat{\gamma}^\vee). \quad (\text{B.28})$$

B.6.2 Error dynamics

Navigation states Because of the semi-direct product structure related to the rotation and velocity states and the corresponding bias states, the derivation of the error dynamics of the $\mathbf{HG}(3)$ part is similar to the one in TG-EqF. In this case, one has

$$\begin{aligned} \dot{e}_R &= \varepsilon_{b_\omega}, \\ \dot{e}_v &= \varepsilon_{b_a} + \mathbf{g}^\wedge \varepsilon_R. \end{aligned}$$

For the position error $\dot{e}_p = \dot{\varepsilon}_p + \mathcal{O}(\varepsilon^2)$, one has

$$\begin{aligned} \dot{e}_p &= \frac{d}{dt}(-\mathbf{R}\hat{\mathbf{R}}^\top \hat{\mathbf{p}} + \mathbf{p}) \\ &= -\dot{e}_R \hat{\mathbf{p}} - e_R \dot{\hat{\mathbf{p}}} + \dot{\mathbf{p}} \\ &= e_R e_{b_\omega}^\wedge \hat{\mathbf{p}} - e_R \hat{\mathbf{v}} + \mathbf{v} \\ \dot{e}_p &= ((\mathbf{I} + \varepsilon_R^\wedge + \mathcal{O}(\varepsilon^2))(\varepsilon_{b_\omega}^\wedge + \mathcal{O}(\varepsilon^2)) \hat{\mathbf{p}} + (\varepsilon_v + \mathcal{O}(\varepsilon^2))) \\ &= \varepsilon_v + \hat{\mathbf{p}}^\wedge \varepsilon_{b_\omega} + \mathcal{O}(\varepsilon^2). \end{aligned}$$

Bias states The derivation of bias error dynamics is the same as TG-EqF, and yields:

$$\dot{e}_b = \text{ad}_{\text{Ad}_{\hat{B}}^\vee \mathbf{w} + \hat{\gamma}^\vee + \mathbf{G}^\vee}^\vee \varepsilon_b + \mathcal{O}(\varepsilon^2).$$

Note that the following relation holds

$$\text{Ad}_{\hat{B}}^\vee \mathbf{w} + \hat{\gamma}^\vee = \Pi(\hat{\mathbf{w}}^\wedge)^\vee,$$

B.6.3 Filter design

The linearized error state matrix $\mathbf{A}_t^0 | \dot{e} \simeq \mathbf{A}_t^0 \varepsilon$ is defined according to

$$\mathbf{A}_t^0 = \begin{bmatrix} \vdots & & & & & \\ 2\mathbf{A} & & & & & \\ \vdots & & \mathbf{I}_6 & & & \\ & \hat{\mathbf{p}}^\wedge & & \mathbf{0}_{3 \times 3} & & \\ \vdots & & & & & \\ \mathbf{0}_{6 \times 9} & \text{ad}_{\text{Ad}_{\hat{B}}^\vee \mathbf{w} + \hat{\gamma}^\vee + \mathbf{G}^\vee}^\vee & & & & \end{bmatrix} \in \mathbb{R}^{15 \times 15}, \quad (\text{B.29})$$

When comparing \mathbf{A}_t^0 in Equ. (B.29) with the one in Equ. (B.18), it is trivial to see the only difference between the two matrices is in the row of \mathbf{A}_t^0 relative to the position error. This is where the major difference between filters employing the symmetries \mathbf{G}_{TF} , and \mathbf{G}_{SD} is found.

Position measurements formulated according to Equ. (34) are equivariant, yielding the following output matrix

$$\mathbf{C}^* = \begin{bmatrix} \frac{1}{2} (y + \hat{\mathbf{p}})^\wedge & \mathbf{0}_{3 \times 3} & -\mathbf{I}_3 & \mathbf{0}_{3 \times 6} \end{bmatrix} \in \mathbb{R}^{3 \times 15}. \quad (\text{B.30})$$

B.7 TFG-IEKF

B.7.1 Overview

The state space is defined as $\mathcal{M} := \mathcal{SE}_2(3) \times \mathbb{R}^6$ with $\xi := (\mathbf{T}, \mathbf{b}) \in \mathcal{M}$. One has $\mathbf{T} = (\mathbf{R}, \mathbf{v}, \mathbf{p}) \in \mathcal{SE}_2(3)$ and $\mathbf{b} = (\mathbf{b}_\omega, \mathbf{b}_a) \in \mathbb{R}^6$. Choose the origin to be $\hat{\xi} = (\mathbf{I}_5, \mathbf{0}_{6 \times 1}) \in \mathcal{M}$. The velocity input is given by $u := (\boldsymbol{\omega}, \mathbf{a}, \boldsymbol{\tau}_\omega, \boldsymbol{\tau}_a)$.

The symmetry group of TFG-IEKF is given by $\mathbf{G}_{\text{TF}} : \mathbf{SO}(3) \ltimes (\mathbb{R}^6 \oplus \mathbb{R}^6)$. Define the filter state $\hat{X} = (\hat{C}, \hat{\gamma}) \in \mathbf{G}_{\text{TF}}$ with $\hat{C} = (\hat{A}, (\hat{a}, \hat{b})) \in \mathbf{SE}_2(3) = \mathbf{SO}(3) \ltimes \mathbb{R}^6$ and $\hat{\gamma} = (\hat{\gamma}_\omega, \hat{\gamma}_a) \in \mathbb{R}^6$. The state estimate is given by

$$\hat{\xi} := \phi(\hat{X}, \hat{\xi}) = (\hat{C}, \hat{A}^{-1} * (-\hat{\gamma})) = (\hat{\mathbf{T}}, \hat{\mathbf{b}}). \quad (\text{B.31})$$

The state error is defined as

$$e := \phi(\hat{X}^{-1}, \xi) = (\mathbf{T}\hat{C}^{-1}, \hat{A} * (\mathbf{b} + \hat{A}^{-1} * \hat{\gamma})) \quad (\text{B.32})$$

$$= (\mathbf{T}\hat{\mathbf{T}}^{-1}, \hat{\mathbf{R}} * (\mathbf{b} - \hat{\mathbf{b}})). \quad (\text{B.33})$$

B.7.2 Error dynamics

Navigation states Because of the semi-direct product structure related to the rotation state, the error dynamics of the rotation part is similar to the TG-EqF,

but with different signs due to the use of log-coordinates $\varepsilon = \log_{\mathbf{G}}$:

$$\dot{\varepsilon}_R = -\varepsilon_{b_\omega}.$$

For the velocity error $e_v = -\mathbf{R} \hat{\mathbf{R}}^\top \hat{\mathbf{v}} + \mathbf{v}$, one has

$$\begin{aligned} \dot{e}_v &= -\dot{e}_R \hat{\mathbf{v}} - e_R \dot{\hat{\mathbf{v}}} + \dot{\mathbf{v}} \\ &= e_R (e_{b_\omega})^\wedge \hat{\mathbf{v}} - e_R \hat{\mathbf{R}}(\mathbf{a} - \hat{\mathbf{b}}_a) - e_R \mathbf{g} + \mathbf{R}(\mathbf{a} - \mathbf{b}_a) + \mathbf{g} \\ &= e_R (e_{b_\omega})^\wedge \hat{\mathbf{v}} - e_R \hat{\mathbf{R}}(\mathbf{a} - \hat{\mathbf{b}}_a) - (e_R - \mathbf{I}) \mathbf{g} \\ &\quad + e_R \hat{\mathbf{R}}(\mathbf{a} - \hat{\mathbf{R}}^\top (e_{b_a} - \gamma_{b_a})) \\ &= e_R e_{b_\omega}^\wedge \hat{\mathbf{v}} - e_R e_{b_a} - (e_R - \mathbf{I}) \mathbf{g}; \\ \dot{e}_v &= -\hat{\mathbf{v}}^\wedge \varepsilon_{b_\omega} + \mathbf{g}^\wedge \varepsilon_R - \varepsilon_{b_a} + \mathcal{O}(\varepsilon^2). \end{aligned}$$

The derivation for position error $e_p = -\mathbf{R} \hat{\mathbf{R}}^\top \hat{\mathbf{p}} + \mathbf{p}$ is similar to the SD-EqF, and it is given by

$$\dot{e}_p = \varepsilon_v - \hat{\mathbf{p}}^\wedge \varepsilon_{b_\omega} + \mathcal{O}(\varepsilon^2).$$

Bias states The error in bias state b_ω is given by $e_{b_\omega} = \hat{\mathbf{R}} * (\mathbf{b}_\omega - \hat{\mathbf{b}}_\omega)$. The dynamics can be derived:

$$\begin{aligned} \dot{e}_{b_\omega} &= \hat{\mathbf{R}}(\omega - \hat{\mathbf{b}}_\omega)^\wedge * (\mathbf{b}_\omega - \hat{\mathbf{b}}_\omega) \\ &= \hat{\mathbf{R}}(\omega - \hat{\mathbf{b}}_\omega)^\wedge \hat{\mathbf{R}}^\top \hat{\mathbf{R}} * (\mathbf{b}_\omega - \hat{\mathbf{b}}_\omega) \\ &= (\hat{\mathbf{R}}(\omega - \hat{\mathbf{b}}_\omega))^\wedge e_{b_\omega}. \end{aligned}$$

In local coordinates, the linearization is given by

$$\dot{e}_{b_\omega} = (\hat{\mathbf{R}}(\omega - \hat{\mathbf{b}}_\omega))^\wedge \varepsilon_{b_\omega} + \mathcal{O}(\varepsilon^2).$$

The error in b_a follows the same derivation, which is given by

$$\dot{e}_{b_a} = (\hat{\mathbf{R}}(\omega - \hat{\mathbf{b}}_\omega))^\wedge \varepsilon_{b_a} + \mathcal{O}(\varepsilon^2).$$

B.7.3 Filter design

The linearized error state matrix $\mathbf{A}_t^0 \mid \dot{\varepsilon} \simeq \mathbf{A}_t^0 \varepsilon$ is defined according to

$$\mathbf{A}_t^0 = \begin{bmatrix} \vdots & -\mathbf{I}_3 & \mathbf{0}_{3 \times 3} \\ {}_4\mathbf{A} & -\hat{\mathbf{v}}^\wedge & -\mathbf{I}_3 \\ \vdots & -\hat{\mathbf{p}}^\wedge & \mathbf{0}_{3 \times 3} \\ \dots & \dots & \dots \\ \mathbf{0}_{3 \times 9} & (\hat{\mathbf{R}}(\omega - \hat{\mathbf{b}}_\omega))^\wedge & \mathbf{0}_{3 \times 3} \\ \mathbf{0}_{3 \times 9} & \mathbf{0}_{3 \times 3} & (\hat{\mathbf{R}}(\omega - \hat{\mathbf{b}}_\omega))^\wedge \end{bmatrix} \in \mathbb{R}^{15 \times 15}. \quad (\text{B.34})$$

Position measurements formulated according to Equ. (34) are equivariant, yielding the following output matrix

$$\mathbf{C}^* = \begin{bmatrix} \frac{1}{2} (y + \hat{\mathbf{p}})^\wedge & \mathbf{0}_{3 \times 3} & -\mathbf{I}_3 & \mathbf{0}_{3 \times 6} \end{bmatrix} \in \mathbb{R}^{3 \times 15}. \quad (\text{B.35})$$

References

- [1] A Barrau and S Bonnabel. The Invariant Extended Kalman Filter as a Stable Observer. *IEEE Transactions on Automatic Control*, 62(4):1797–1812, 2017.
- [2] Axel Barrau and Axel Barrau. *Non-linear state error based extended Kalman filters with applications to navigation*. PhD thesis, Mines Paristech, 9 2015.
- [3] Axel Barrau and Silvere Bonnabel. A Mathematical Framework for IMU Error Propagation with Applications to Preintegration. *Proceedings - IEEE International Conference on Robotics and Automation*, pages 5732–5738, 5 2020.
- [4] Axel Barrau and Silvere Bonnabel. The Geometry of Navigation Problems. *IEEE Transactions on Automatic Control*, 68(2):689–704, 2022.
- [5] Christian Brommer, Alessandro Fornasier, Martin Scheiber, Jeff Delaune, Roland Brockers, Jan Steinbrener, and Stephan Weiss. The INSANE dataset: Large number of sensors for challenging UAV flights in Mars analog, outdoor, and out-/indoor transition scenarios. *International Journal of Robotics Research*, 2 2024.
- [6] Martin Brossard, Axel Barrau, Paul Chauchat, and Silvere Bonnabel. Associating Uncertainty to Extended Poses for on Lie Group IMU Preintegration With Rotating Earth. *IEEE Transactions on Robotics*, 38(2):998–1015, 2021.
- [7] Michael Burri, Janosch Nikolic, Pascal Gohl, Thomas Schneider, Joern Rehder, Sammy Omari, Markus W. Achtelik, and Roland Siegwart. The EuRoC micro aerial vehicle datasets. <https://doi.org/10.1177/0278364915620033>, 35(10):1157–1163, 1 2016.
- [8] Gregory S Chirikjian. *Stochastic models, information theory, and Lie groups, volume 2: Analytic methods and modern applications*, volume 2. Springer Science & Business Media, 2011.
- [9] Alessandro Fornasier, Pieter van Goor, Eren Alak, Robert Mahony, and Stephan Weiss. MSCEqF: A Multi State Constraint Equivariant Filter for Vision-aided Inertial Navigation. *IEEE Robotics and Automation Letters*, 1 2023.
- [10] Alessandro Fornasier, Yonhon Ng, Christian Brommer, Christoph Bohm, Robert Mahony, and Stephan Weiss. Overcoming Bias: Equivariant Filter Design for Biased Attitude Estimation With Online Calibration. *IEEE Robotics and Automation Letters*, 7(4):12118–12125, 10 2022.
- [11] Alessandro Fornasier, Yonhon Ng, Robert Mahony, and Stephan Weiss. Equivariant Filter Design

- for Inertial Navigation Systems with Input Measurement Biases. *2022 International Conference on Robotics and Automation (ICRA)*, pages 4333–4339, 5 2022.
- [12] Yixiao Ge, Pieter Van Goor, and Robert Mahony. A Geometric Perspective on Fusing Gaussian Distributions on Lie Groups. *IEEE Control Systems Letters*, 8:844–849, 2024.
- [13] Ross Hartley, Maani Ghaffari, Ryan M Eustice, and Jessy W Grizzle. Contact-aided invariant extended Kalman filtering for robot state estimation. *The International Journal of Robotics Research*, 39(4):402–430, 2020.
- [14] Simon J. Julier and Joseph J. LaViola. On Kalman filtering with nonlinear equality constraints. *IEEE Transactions on Signal Processing*, 55(6 II):2774–2784, 6 2007.
- [15] E. J. Lefferts, F. L. Markley, and M. D. Shuster. Kalman Filtering for Spacecraft Attitude Estimation. <https://doi.org/10.2514/3.56190>, 5(5):417–429, 5 1982.
- [16] X. Rong Li, Zhanlue Zhao, and Xiao Bai Li. Evaluation of Estimation Algorithms: Credibility Tests. *IEEE Transactions on Systems, Man, and Cybernetics Part A: Systems and Humans*, 42(1):147–163, 2012.
- [17] Xinghan Li, Haodong Jiang, Xingyu Chen, He Kong, and Junfeng Wu. Closed-Form Error Propagation on SE-n (3) Group for Invariant EKF With Applications to VINS. *IEEE Robotics and Automation Letters*, 7(4):10705–10712, 10 2022.
- [18] Robert Mahony, Tarek Hamel, and Jochen Trunpf. Equivariant Systems Theory and Observer Design. *arXiv preprint arXiv:2006.08276*, 6 2020.
- [19] Robert Mahony, Jochen Trunpf, and Tarek Hamel. Observers for kinematic systems with symmetry? *IFAC Proceedings Volumes (IFAC-PapersOnline)*, 9(PART 1):617–633, 2013.
- [20] Robert Mahony, Pieter Van Goor, and Tarek Hamel. Observer Design for Nonlinear Systems with Equivariance. <https://doi.org/10.1146/annurev-control-061520-010324>, 5:221–252, 5 2022.
- [21] Yonhon Ng, Pieter Van Goor, Tarek Hamel, and Robert Mahony. Equivariant Systems Theory and Observer Design for Second Order Kinematic Systems on Matrix Lie Groups. *Proceedings of the IEEE Conference on Decision and Control*, 2020-Decem(Xx):4194–4199, 2020.
- [22] Yonhon Ng, Pieter van Goor, and Robert Mahony. Pose Observation for Second Order Pose Kinematics. *IFAC-PapersOnLine*, 53(2):2317–2323, 1 2020.
- [23] Yonhon Ng, Pieter Van Goor, Robert Mahony, and Tarek Hamel. Attitude Observation for Second Order Attitude Kinematics. In *Proceedings of the IEEE Conference on Decision and Control*, volume 2019-Decem, pages 2536–2542. IEEE, 2019.
- [24] Natalia Pavlasek, Alex Walsh, and James Richard Forbes. Invariant Extended Kalman Filtering Using Two Position Receivers for Extended Pose Estimation. In *2021 IEEE International Conference on Robotics and Automation (ICRA)*, pages 5582–5588. Institute of Electrical and Electronics Engineers (IEEE), 10 2021.
- [25] Martin Scheiber, Alessandro Fornasier, Christian Brommer, and Stephan Weiss. Revisiting Multi-GNSS Navigation for UAVs – An Equivariant Filtering Approach. In *2023 21st International Conference on Advanced Robotics (ICAR)*, pages 134–141. IEEE, 12 2023.
- [26] Joan Solà. Quaternion kinematics for the error-state Kalman filter. *arXiv preprint arXiv:1711.02508*, 11 2017.
- [27] Pieter Van Goor. *Equivariant Filters for Visual Spatial Awareness*. PhD thesis, Australian National University (ANU), 2023.
- [28] Pieter Van Goor, Tarek Hamel, and Robert Mahony. Equivariant Filter (EqF): A General Filter Design for Systems on Homogeneous Spaces. *Proceedings of the IEEE Conference on Decision and Control*, 2020-Decem(Cdc):5401–5408, 2020.
- [29] Pieter van Goor, Tarek Hamel, and Robert Mahony. Equivariant Filter (EqF). *IEEE Transactions on Automatic Control*, 68(6):3501 – 3512, 6 2022.